Migration of Massive Planets

Dissertation
der Mathematisch-Naturwissenschaftlichen Fakultät
der Eberhard Karls Universität Tübingen
zur Erlangung des Grades eines
Doktors der Naturwissenschaften
(Dr. rer. nat.)

vorgelegt von
Christoph Dürmann
aus Oberhausen

Tübingen
2017

Tag der mündlichen Qualifikation:	27.04.2017
Dekan:	Prof. Dr. Wolfgang Rosenstiel
1. Berichterstatter:	Prof. Dr. Wilhelm Kley
2. Berichterstatter:	Prof. Dr. Klaus Werner

Science is a way of trying not to fool yourself.

RICHARD FEYNMAN

Zusammenfassung

Diese Arbeit beschäftigt sich mit der Migration von massereichen Planeten mit einer Planetenmasse von $M_\mathrm{P} \gtrsim 0.5 M_\mathrm{Jupiter}$. Planetenmigration bezeichnet die Veränderung der großen Halbachse des Orbits eines Planeten. Die Gravitationskräfte von durch den Planeten verursachten Störungen in der Scheibe bewirken ein Drehmoment, welches den Drehimpuls des Planeten verändert, wodurch sich dessen Orbit verkleinert oder vergrößert. Diese massereichen Planeten öffnen dabei eine ringförmige Lücke in der Gasscheibe. Diese bewirkt, dass die Drehmomente abnehmen und der Planet langsamer migriert. Gleichzeitig hat die verringerte Dichte in der Nähe des Planeten Auswirkungen auf sein Wachstum.

Im Rahmen dieser Arbeit und der eingebetteten Publikationen wurden numerische Simulationen durchgeführt, um für verschiedene Parameter wie Dichte der Scheibe, Masse des Planeten, Stärke der Viskosität und der Akkretionsrate das genaue Verhalten zu untersuchen. Die Ergebnisse zeigen, dass sich Typ II Migration nicht so verhält wie bisher verwendete einfache Modelle nahelegen. Die Migrationsrate hängt von den genauen Eigenschaften der Scheibe ab und entspricht nicht einfach der viskosen radialen Strömungsgeschwindigkeit, die in diesen Modellen sowohl unter- als auch überschritten werden kann. Grund dafür ist, dass die Lücke in der Scheibe nicht geeignet ist die innere von der äußeren Scheibe zu trennen, da Gas die Lücke in beide Richtungen passieren kann. Dies ist auch für akkretierende Planeten unter bestimmten Umständen noch der Fall.

Die Simulationen zeigen auch, dass die Migrationsrate und die Akkretionsrate des Planeten miteinander wechselwirken. Schneller migrierende Planeten können, da mehr Gas die Lücke passieren muss, schneller wachsen. Gleichzeitig sorgt Akkretion für eine tiefere Lücke, wodurch die Drehmomente in der direkten Umgebung des Planeten reduziert werden und die Migrationsrate sinkt.

Für Modelle, die Typ II Migration untersuchen sollen, ist also eine gleichzeitige Berücksichtigung beider Effekte notwendig. Unter geeigneten Bedingungen könnte so die Migration verlangsamt werden, um bestehende Probleme bei der Entstehung von Gasriesenplaneten zu lösen.

Abstract

This thesis studies the migration of massive planets with mass $M_P \gtrsim 0.5 M_{Jupiter}$. Planetary migration is a process that changes the semi-major axis of the planetary orbit. The gravitational forces of disturbances in the disk density created by the planet result in a torque changing the angular momentum of the planet and thus reducing or increasing its distance to the star. Planets this massive also open an annular gap in the disk. Because of the gap the torques close to the planet are reduced resulting in a slowdown of the migration. At the same time the reduced density due to the gap will have effects on the growth of the planet.

For this work and the embedded publications numerical simulations were conducted with different parameters as disk density, planet mass, strength of viscosity and accretion rate in order to study the migrational behavior in detail. The results show that type II migration is not working as the simple models used today suggest. The migration rate depends on the exact properties of the disk and is not just the viscous radial speed of the gas which can be slower or faster than the migration in this models. The reason is that the gap is not able to separate the inner from the outer disk because gas can cross the gap in both directions. Even though, accretion onto the planet will not prohibit gas crossing the planet's orbit.

Furthermore, the simulations show the migration and accretion rate depend mutually on each other. Planets migrating faster can accrete more gas because more gas must cross the gap. At the same time accretion leads to a deeper gap which then reduces the torques from the region close to the planet and this way leads to slower migration.

Hence, to study type II migration in numerical models both migration and accretion should be considered at the same time. Under certain circumstances this might slow down migration and thus solve current problems of giant gas planet formation.

Contents

1 Introduction

1.1 The Solar System

Planets are the biggest bodies in the Solar System apart from the Sun itself. The name *planet* derives from the ancient Greek term for wandering star, because planets appear like stars in the sky but move differently than stars do. The six inner planets Mercury, Venus, Earth, Mars, Jupiter and Venus were already known to Babylonian astronomers in the 7th century BC (Hunger et al. 1992), although of course Earth was not considered to be the same kind of object as the other five planets. These planets were easy to distinguish from the star background because they move in distinct shapes across the sky and they are at least at certain times much brighter than most stars. Only after the invention of the telescope it became possible to detect the other planets Uranus (W. Herschel, 1781), Neptune (J. G. Galle, 1846) and Pluto (Tombaugh, 1930).

In recent years more objects similar to Pluto were found (Eris, Makemake, Haumea) which caused debate whether Pluto should be called a planet. In 2006 the International Astronomical Union (IAU) defined a new class of *dwarf planets* in which the mentioned objects including Pluto are now classified. The IAU officially defined what is considered to be a planet in the Solar System as follows (General Assembly of the IAU 2006):

> A ”planet” is a celestial body that
>
> (a) is in orbit around the Sun,
>
> (b) has sufficient mass for its self-gravity to overcome rigid body forces so that it assumes a hydrostatic equilibrium (nearly round) shape, and
>
> (c) has cleared the neighborhood around its orbit.

Planets outside the Solar System instead must orbit a star or stellar remnant and in addition must not be massive enough to cause thermonuclear fusion in their interior.

When Voyager 2 performed a fly-by at Neptune in August 1989 probes from Earth had visited all Solar System planets and in July 2015 the New Horizons spacecraft took the

planet	diameter 1000 km	mass $M_\oplus$	semi-major axis au	orbital period years	inclination °	eccentricity
Mercury	4.87	0.06	0.39	0.24	3.38	0.216
Venus	12.11	0.82	0.72	0.62	3.86	0.007
Earth	12.76	1.00	1.00	1.00	7.25	0.017
Mars	6.79	0.11	1.52	1.88	5.65	0.093
Jupiter	142.99	317.80	5.20	11.86	6.09	0.048
Saturn	120.53	95.20	9.54	29.46	5.51	0.054
Uranus	51.11	14.60	19.22	84.01	6.48	0.047
Neptune	49.53	17.20	30.06	164.80	6.43	0.009

Table 1.1: Orbital and physical properties of the planets in the Solar System.

first high resolution images of Pluto and its moon Charon. Probes landed on Venus and Mars and entered the atmosphere of Jupiter. Due to these missions and the possibility to observe the planets directly with telescopes from Earth and Earth orbit, we have a good understanding of the planet's orbits, their basic physical properties (radius, mass) and the composition of their crust and/or atmosphere.

It is much more difficult to learn about the inner structure of these bodies. On Earth, we can get information about the interior by seismic measurements but this is much more complicated for the other planets because this is not possible from orbit. Some results can be obtained from measuring the gravitational potential very accurately but this is not easy in itself. All this knowledge is needed to understand how the planets in the Solar System might have formed.

1.2 Protoplanetary disks

Protoplanetary disks are the astronomical objects in which planets and planetary systems form. They are a by-product of star formation which itself is a result of molecular clouds collapsing under their own gravity. Most stars form in a *giant molecular cloud* (GMC) which is a region with a typical diameter of 50 pc and a mass of $10^5\,M_\odot$. Typical temperatures are $T \sim 50\,\mathrm{K}$ and the number densities range between $n \sim 1 \times 10^8$ to $3 \times 10^8\,\mathrm{m}^{-3}$ but in *dense cores*, regions of around $10\,M_\odot$ and characteristic diameters of 0.1 pc, temperatures can be even lower at around 10 K and densities higher by a factor

of 100. The *Jeans criterion* defines the Jeans mass M_J which the cloud mass M_C has to exceed to overcome thermal pressure and to collapse,

$$M_\mathrm{C} > M_\mathrm{J} \simeq \left(\frac{5kT}{G\mu m_\mathrm{H}}\right)^{3/2} \left(\frac{3}{4\pi\rho_0}\right)^{1/2}, \tag{1.1}$$

where k is the Boltzmann constant, G the gravitational constant, μ the mean molecular weight, m_H the mass of the hydrogen atom, and T and ρ_0 the temperature and density of the cloud. For dense cores the Jeans criterion is fulfilled so that these regions may collapse to form one or more new stars. Usually a dense core will form multiple protostars which mutually interact and also might end up as binary or multiple star systems. To explain the general process of planetary system formation we focus on one star and assume interactions with this star occur only at great distances and they therefore do not interfere with the gaseous disk around the star.

The gas in the collapsing region of the giant molecular cloud will have small random velocities leading to a non-zero angular momentum. As the collapsing gas cloud shrinks angular momentum is conserved and therefore the gas is beginning to rotate faster and faster. The collapse can no longer be spherical but will form a flat rotating structure, a disk. Only by transfer of angular momentum from the inner to the outer parts of the disk the gas can be accreted onto the star. Because the transport of angular momentum depends on the viscosity of the gas and accretion is coupled to this momentum transport the accretion rate depends on the viscosity in the disk. The most obvious source of viscosity is molecular viscosity. The molecular viscosity of a typical hydrogen helium mixture in a protoplanetary disk will be of the order $v_\mathrm{m} \sim 10^7\,\mathrm{cm^2 s^{-1}}$ (Armitage 2010, p. 79). Because the released gravitational energy heats up the accreted gas it can be observed as *infrared excess* of young stars with disks. From these observations, the accretion rate of the disk as a function of the age of the star can be estimated as done by Hartmann et al. (1998). They found the accretion rate to be in the range of 10^{-9} to $10^{-7}\,M_\odot$/yr at the age of 1 Myr. With the gas surface density at 1 au in a protoplanetary disk able to form the Solar System being on the order of $1000\,\mathrm{g\,cm^{-2}}$ (Hayashi 1981; Desch 2007) and the molecular viscosity (see above) the estimate for the accretion rate is

$$\dot{m} = 2\pi r u_r \Sigma \approx -3\pi\nu\Sigma \approx -2 \times 10^{-15}\,M_\odot/\mathrm{yr}, \tag{1.2}$$

where u_r is the radial velocity of the gas, Σ the surface density and ν the viscosity. This value is too small by at least 6 orders of magnitude. This means there must be other sources of viscosity than only the molecular viscosity. To overcome this problem vis-

cosity is parameterized in the form $v = \alpha c_s H$ where H is the disk scale height, c_s is the speed of sound and α a free parameter (Shakura & Sunyaev 1973). Simulations show that this parameter is on the order of 10^{-3} for protoplanetary disks. As physical sources different hydrodynamical and magneto-hydrodynamical instabilities such as the magnetorotational instability (MRI) (Balbus & Hawley 1991) and the vertical shear instability (VSI) (Nelson et al. 2013; Stoll & Kley 2014) are discussed.

By observing young stellar clusters and looking for the fraction of stars with disks the typical lifetime of protoplanetary accretion disks can be estimated. Haisch et al. (2001) found the typical lifetime of a disk to be $\tau_{\text{disk}} \approx 2.4\,\text{Myr}$. This sets a limit for the time available to form giant planets consisting mostly of gas as these planets must have reached their final masses before the disk vanishes. There are multiple mechanisms which can lead to disk dissipation. One factor is of course the accretion onto the central star and to a much smaller extent the accretion by gas planets. As angular momentum has to be transported outwards in the accretion process and angular momentum has to be carried by some material a part of the gas is also lost to the interstellar medium. Late protoplanetary disks which are in the phase of dissipation are called transition disks. Observations show only very few transitions disks which means that disk dissipation must be a very rapid process with time scales on the order of 10 % of the disk lifetime (Skrutskie et al. 1990; Cieza et al. 2007). Because accretion seems to be too slow to achieve such short timescales a process called photoevaporation is discussed (Owen et al. 2011). Photoevaporation creates disk winds carrying away gas from the disk and which are driven by the X-ray and EUV luminosity of the young star.

1.3 Planet formation

1.3.1 Terrestrial planets

Terrestrial planets are also called rocky planets, because they mainly consist of solid material like silicates and other heavy elements. The terrestrial planets in the Solar System are the inner planets Mercury, Venus, Earth and Mars. This type of planets are of special interest for planetary science as it is thought that only these planets can provide conditions for the genesis of extraterrestrial life.

Formation of planetary cores is a very complicated and still not completely understood process and thus it is not possible to give a complete overview of the current models

here. Therefore only a very brief overview is given here as a more complete picture can be found in recent review papers (Raymond et al. 2014; Johansen et al. 2014).

Terrestrial planets must form from solid particles in the disk as silicates or ices. The mass fraction of solids in a protoplanetary disk is thought to be on the order of 1 % (Hayashi 1981). Small dust particles are coupled to the gas but as the dust coagulates to bigger aggregates it decouples. From the size of the particles the typical differential velocities can be calculated (Weidenschilling & Cuzzi 1993). When the particles do no longer move with the gas they are more likely to collide with each other which can lead to growth. Until the objects reach a size of $\sim$ 1 km gravitation is not important but later it can enhance the collision cross section. Subsequent collisions and impacts then form planetesimals, objects bigger than $\sim$ 10 km. The first planetesimals that reach even larger diameters will sweep through the disk and collect smaller bodies and thus grow to planetary mass. Because only few objects which reach high enough masses first can grow this way this is called oligarchic growth.

1.3.2 Gas planets

There are two main hypotheses how giant gas planets form. A planet could form in the disk by gravitational collapse just like a star forms in a molecular cloud which is called *gravitational instability* (GI). The other idea is that a rocky planet forms first and as it becomes massive enough it can start to accrete gas from the disk which is called *core accretion*.

The conditions needed to form planets by gravitational instability can be found with the *Toomre criterion* (Toomre 1964) which is needed for a gaseous disk to be stable against axisymmetric perturbations,

$$Q = \frac{c_s \kappa}{\pi G \Sigma} > 1. \tag{1.3}$$

In this expression κ is the epicyclic frequency, G is Newton's gravitational constant and Σ the surface density of the disk. The Jeans criterion is not applicable because a disk is rotating and therefore shear forces must be considered. Obviously the Toomre parameter Q is a local quantity and has to be evaluated for every region of the disk. Where $Q < 1$ the disk can be unstable and form fragments if the disk is able to cool fast enough because the release of gravitational energy causes the gas to heat up (Gammie 2001). Therefore, the surface density must be high while the temperature is low to reduce the speed of sound. The epicyclic frequency is, in case of Keplerian rotation, just the orbital

frequency which reduces with distance from the star. So planet formation by gravitational instability can only happen far away from the central star at distances of more than $60 - 100$ au (Matzner & Levin 2005; Rafikov 2009).

The other model to form giant planets is based on the formation of rocky planetary cores which start to accrete gas from the disk. This process is initially the same as in the formation process of terrestrial planets. Around the core gas is bound in a hydrostatic envelope extending out to the Bondi radius. The Bondi radius,

$$R_\mathrm{B} = \frac{2GM_\mathrm{P}}{c_\mathrm{s}^2}, \tag{1.4}$$

gives the distance from the planet with mass M_P at which the sound speed c_s is equal to the escape velocity $v_\mathrm{e} = \sqrt{2GM/r}$. The gravitational energy released by planetesimals accreted by the planet must be transported through the envelope which becomes non-isothermal. Its mass increases and when it dominates the planet's mass the accretion rate is no longer limited by the supply of planetesimals but gas can be accreted. Gas accretion is limited by how fast the planet can cool away the excess heat from the gravitational energy released in the process. This phase is called *runaway accretion* because it is usually much faster than the initial growth. Considering the energy transfer inside the envelope the critical core mass needed to enter the runaway accretion regime is around $10\,M_\oplus$ (Mizuno 1980). It then takes only on the order of 10^5 years for the planet to reach its final mass.

Why and at which time accretion finally stops is still an open problem. One explanation is that the disk dissolves, for example by photoevaporation (Shu et al. 1993), and thus there is no more gas feeding the planet. Another idea is that the planet, as it becomes more and more massive, starts to open a gap in the gas disk (Ward 1982) and this way limits the amount of gas available for growth.

1.4 Exoplanets

The Solar System is just one single system of planets around one star. It cannot give any insight what a typical planetary system might look like. However, the most important way to couple theoretical models to reality is by comparing their outcome to observations. Hence it is necessary to observe planets orbiting other stars. Planets not orbiting the Sun but other stars are called *exoplanets*. The first exoplanets detected (and

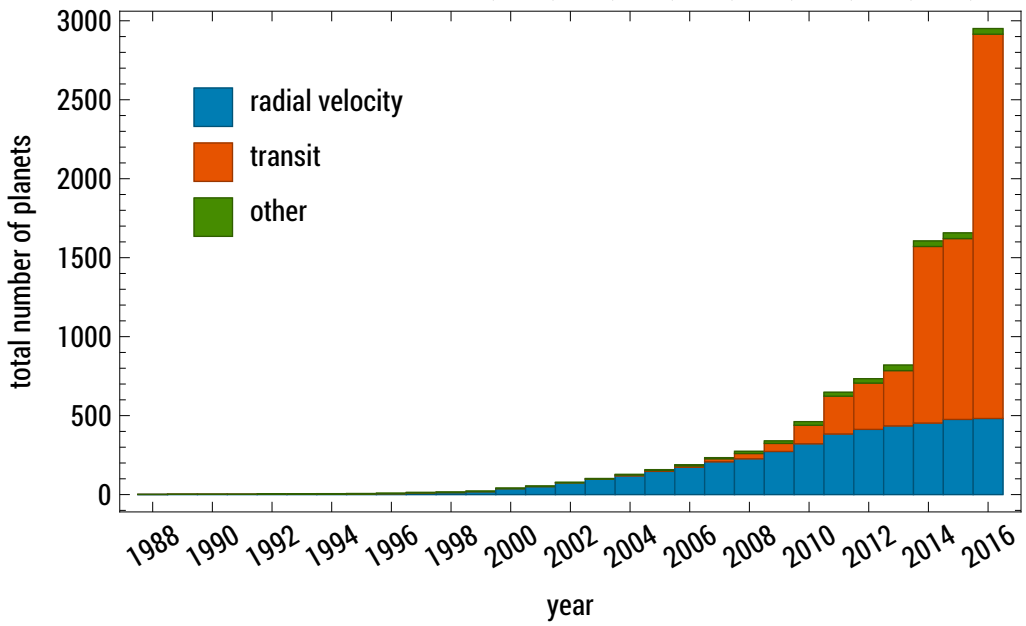

Figure 1.1: All exoplanets known to the time grouped by detection method. (Data from exoplanets.org, 8.11.16)

where the discovery was not later retracted) were three companions to the pulsar PSR B1257+12 found by Wolszczan & Frail (1992). The first substellar companion detected around a main sequence star was an object around HD 114762 by Latham et al. (1989). With a minimum mass of $11\,M_{\mathrm{Jup}}$ it is probably not a planet but a Brown Dwarf. Then in 1995 Mayor & Queloz found an exoplanet with a minimum mass of $0.46\,M_{\mathrm{Jup}}$ around the Sun-like star 51 Pegasi. Since then more than 3000 exoplanets have been detected during the years and the list gets longer every year.

1.4.1 Detection methods

In Fig. 1.1 the number of known planets is shown and coded by color are the methods that were used for these discoveries. The first discoveries were made by measurements of the star's radial velocity.

By measuring the shifting of known absorption lines in stellar spectra the movement of the star along the viewing axis can be measured with very high precision down to the order of 1 m/s. Because the planet and the star are orbiting around their common center of mass the star is moving away from us when the planet is moving in our direction. This

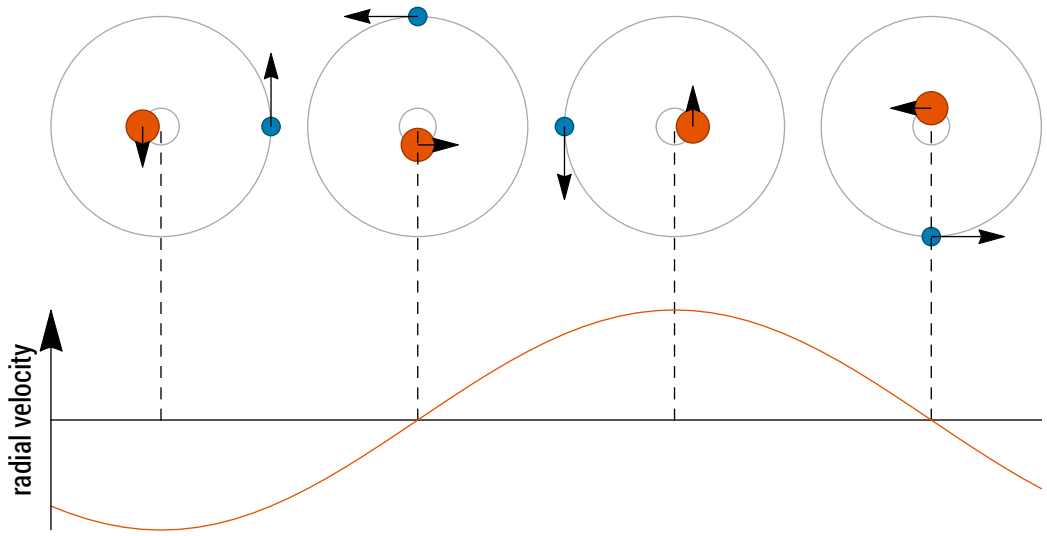

Figure 1.2: Radial velocity method for planet detection. The planet (blue) and the star (red) are orbiting their common center of mass.

is shown in Fig. 1.2. Unfortunately, we can only observe the velocity component along the viewing axis so the effect is biggest in case we see the planet's orbit edge on and invisible in case of a face on alignment. This means, in case of a known stellar mass, the amplitude does not give directly the mass M_P of the planet but $M_P \times \sin i$ where i is the inclination with respect to our direction of view. Only in case of a circular orbit the radial velocity variation resembles a sine function, in case of an eccentric orbit it becomes distorted. This way also the eccentricity can be measured.

Today most planets are detected by transits of the planet in front of its host star. Transits can be measured by photometry, but high accuracy is necessary because for example Jupiter transiting our Sun would only reduce the Sun's luminosity by 1 % and in case of the Earth by only 0.01 %. The depth of the eclipse directly yields the ratio of the planet's radius to the star's radius, but masses have to be determined by other methods like the radial velocity as mentioned before. Because in these cases the inclination is known the exact mass of the planet can be calculated. Combined with the radius even its mean density can be calculated. This is of course very interesting as it gives indications to the planet's composition. Often the stars are too far away and therefore too dim for radial velocity measurements being feasible and the masses can only be estimated by models of planetary compositions and the resulting densities.

Most planets have been detected by the radial velocity or transit method, but a few discoveries were made with different techniques. The naivest method is direct imaging where the planet can be seen directly with telescopes. The main problem is that planets only emit in infrared wavelengths and that the central star is more luminous by many orders of magnitude. For planets only a few au apart from the star there is also the problem that the star overexposes the imaging sensor which makes direct imaging of close planets impossible. The 9 planets in 6 planetary systems detected by direct imaging are either giant planets with multiple Jupiter masses or very far (113 au for Fomalhaut b) away from the star. In all but one case the distance from the Sun to the star is less than 40 pc. With better telescopes like the European Extremely Large Telescope (EELT) with its 30-meter mirror or the Thirty Meter Telescope (TMT) direct imaging might become more viable and would allow not only for planet detection but also and more important for spectroscopic analysis of the atmospheres. Measuring the composition of the atmosphere of an exoplanet is very interesting in order to search for life on other planets but also to constrain planet formation models.

Another method is the detection by gravitational microlensing events. Microlensing occurs when two stars are nearly perfectly aligned and the star closer to the observer is orbited by a planet. The closer star aligns with the star further away due to its transverse motion and because of gravitational lensing the far star appears much brighter, following a distinctive brightness profile. If there is a planet orbiting the closer star and this planet is aligned properly it may create a second small brightness peak. This means that such a detection cannot be repeated and only the current distance to the host star can be measured but not the other orbital properties. Other methods depend on timing very precisely the beginning and/or the duration of eclipses of known planets. From the deviations of the single planet model these transit timing variations allow to detect additional planets in the same system.

1.4.2 Known exoplanets

In Fig. 1.3 all exoplanets known today are shown according to their semi-major axis and their mass (or estimated mass). Some regions in this plot are very densely populated and other regions are void of any planets. This can be because of two reasons: First, there are just no (or very few) planets with that properties, or second, we are not able to detect planets with these properties (yet). The so-called detection bias depends on the detection method and general properties of the planet. Less massive planets are of

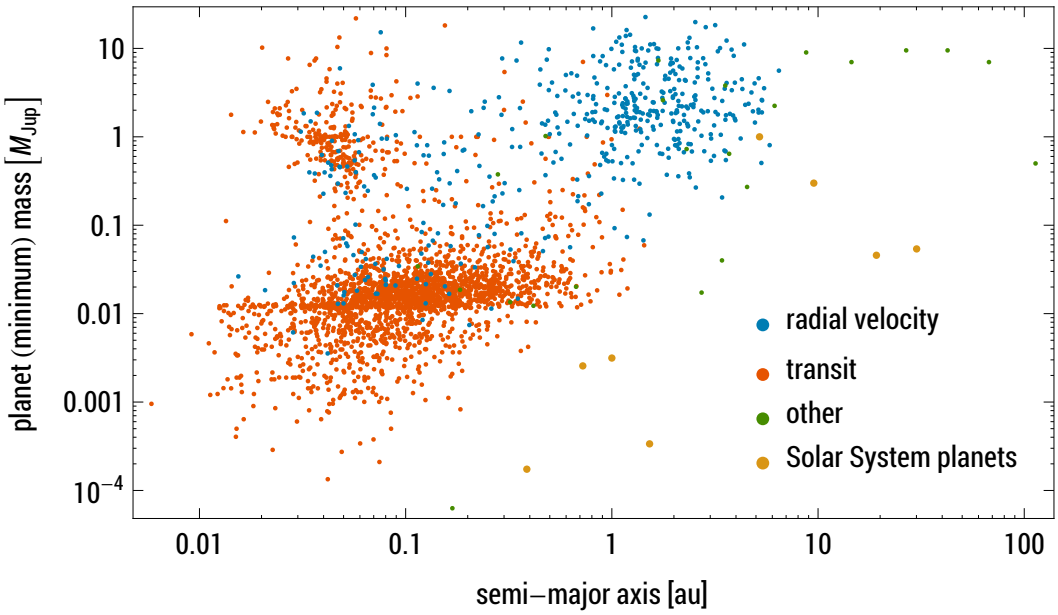

Figure 1.3: Exoplanet population discovered today. Three different clusters can easily be seen. The empty region to the lower right is mostly due to a detection bias.

course harder to detect because the will have a smaller gravitational effect on the star (radial velocity method) and only have weak eclipses (transit method) assuming low mass planets are also small. Apart from limits in sensitivity of the used instruments another important factor is observation time. To confirm a potential detection, it must be observed for at least a full orbit which can lead to very long observation times for planets with large separations form the orbited star. This leads to very few planets found beyond 5 au.

Because of that some planets cannot be detected as easy as others and vice versa some kinds of exoplanets may be overrepresented in our current sample. The transit method favors planets close to the star, because the range of inclinations which still lead to an eclipse directly depends on the distance to the star. It also favors massive and thus bigger planets, because the signal of the eclipse in the luminosity is stronger. Hence, the upper left region in Fig. 1.3 is overpopulated. Planets with a mass of around $1\,M_{\mathrm{Jup}}$ and a semi-major axis of less than 0.1 au are called *hot Jupiters*. They are far closer to their star than Mercury (0.39 au, see Tab. 1.1). Already for 51 Pegasi b, the first hot Jupiter detected (Mayor & Queloz 1995), Lin et al. (1996) proposed it would have

had to migrate inward from initially much greater distances because it could not have formed that close to the star. So even though hot Jupiters are not as common as Fig. 1.3 suggests they still delivered the interesting insight that planets have to migrate.

1.5 Planet migration

Planet migration is a mechanism that changes the semi-major axis of planets by the exchange of angular momentum with the protoplanetary disk. This transfer comes from gravitational forces between the planet and non-axisymmetric regions in the disk. Usually planetary migration is divided into two regimes which are called *type I* and *type II* migration. The first is important for planets with mass $M_\mathrm{P} \lesssim 50 M_\oplus$ and the latter for planets with mass $M_\mathrm{P} \gtrsim \frac{1}{2} M_\mathrm{Jup} = 158 M_\oplus$. There is an intermediate regime which is called *type III* migration.

The following sections give a short overview on the different migration regimes. For further reading it is recommended to have a look at reviews like Kley & Nelson (2012) or Baruteau et al. (2014).

1.5.1 Type I migration

As the gas density in a protoplanetary disk decreases with the distance to the star usually also the pressure decreases. This pressure gradient acts as an additional outward force on the gas leading to a sub-Keplerian rotation which means the gas is orbiting the star slower than Kepler's third law suggests. This pressure force does not act on solid bodies and therefore planets (and other solid objects like dust, planetesimals, etc.) usually are moving faster than the surrounding gas. While small objects like dust will easily couple to the gas flow by drag this is not true for objects with radii R of several hundred kilometers or even more because $F_\mathrm{drag} \propto R^2$ but $M \propto R^3$ and thus the acceleration $a = F/M \propto R^{-1}$. This means planets are not affected by classical gas drag.

As the planet is moving through the disk it is constantly overtaking gas in the outer disk which will be redirected by the gravitational potential of the planet. Lin & Papaloizou (1979) showed with the impulse approximation that gas close to but outside the planets orbit will gain angular momentum and the planet will lose angular momentum. This angular momentum exchange results in spiral waves created by the planet as can be seen in the left panel of Fig. 1.4. The same happens with opposite signs to the gas on

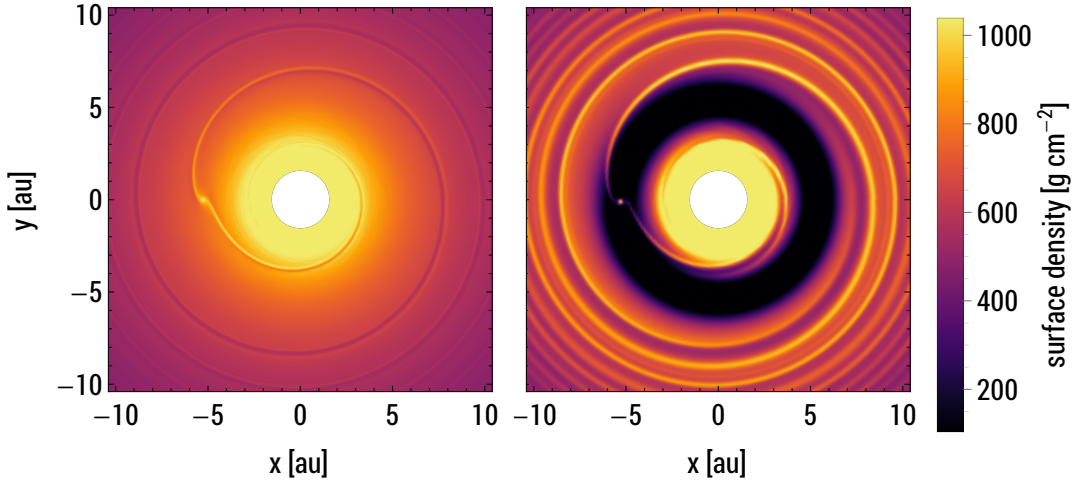

Figure 1.4: Surface density of a $10\,M_\oplus = 0.03\,M_\mathrm{Jup}$ (left) and a $1\,M_\mathrm{Jup}$ planet (right) after disk relaxation to equilibrium. The planet is at 5.2 au left of the central star. The white disk in the center was not part of the computational domain.

a slightly smaller orbit than the planet. If both contributions do not exactly cancel out this will lead to migration. Because there is no underlying physical process that would ensure equal torques from the inner and the outer disk usually the inner or outer torques dominate leading to outward or inward migration, respectively. As long as the planets are not too massive, $M_\mathrm{P} \lesssim 30 M_\oplus$, they can mostly be treated by linear analysis where the torques scale as (Goldreich & Tremaine 1979; Tanaka et al. 2002)

$$\Gamma_0 = \left(\frac{M_\mathrm{P}}{M_*}\right)^2 \left(\frac{H}{r_\mathrm{P}}\right)^{-2} \Sigma_\mathrm{P} r_\mathrm{P}^4 \Omega_\mathrm{P}^2, \tag{1.5}$$

where Ω is the orbital frequency and the index P denotes the value at the position of the planet. The prefactor to this scaling then usually depends on local disk properties as the density gradient and the temperature gradient. The migration timescale $\tau_\mathrm{mig} = a_\mathrm{P}/\dot{a}_\mathrm{P}$ for type I migration of an Earth-like planet around a Solar-type star at 1 au can be as short as 10^5 yr which is much shorter than the disk lifetime.

It is possible that in some regions in the disk and for some planetary masses type I migration is inwards and outwards at other locations. The boundaries of these regions are called *zero-torque radii* because the torque on the planet will vanish there (Bitsch & Kley 2011). This effect could create stable locations at which bodies of similar masses could accumulate.

1.5.2 Type II migration

As can be seen from Eq. 1.5 the torques scale with q^2, where $q = M_P/M_*$ is the mass ratio of the planet to the star, and therefore the migration rate increases as $\dot{a}_P \propto \Gamma/M_P \propto M_P$. For very massive planets migration would become extremely fast as planetary masses cover more than 3 orders of magnitude. This fast migration is prevented as planets start to create a gap in the disk (see Fig. 1.4), an annular region around the planet's orbit where the gas density is reduced and because of the gap the migrational behavior changes. This regime is called type II migration.

The basic principle why a gap forms is the gravitational transfer of angular momentum in the same way as in the case of type I migration. The angular momentum of the planet is carried away in the spiral density waves and as these form shocks the angular momentum is deposited in the disk. Due to the much stronger forces created by a more massive planet the viscosity in the disc is no longer able to dissipate the angular momentum deposited in a small region and the gas will be pushed away from the planet. To form a gap that is wide enough to clear the Hill sphere with a radius of $R_H = (q/3)^{1/3} a_P$ Lin & Papaloizou (1993) formulated the viscous criterion

$$q \gtrsim \frac{40\nu}{a_P^2 \Omega_P}. \tag{1.6}$$

In addition, it is necessary that the Hill radius exceeds the disk scale height because otherwise the gap would be Rayleigh unstable (Lin & Papaloizou 1993). This leads to a thermal criterion because the disk scale height is a measure for the temperature, $H = c_S/\Omega \propto T$. Both were included in the gap opening criterion of Crida et al. (2006),

$$1 \gtrsim \frac{3}{4}\frac{H}{R_H} + \frac{50\nu}{q a_P^2 \Omega_P}, \tag{1.7}$$

which must be fulfilled to form a gap with a relative depth $\Sigma_G/\Sigma_0 \leq 0.1$ where Σ_G is the surface density in the gap and Σ_0 is the undisturbed surface density. For more massive planets the relative surface density can be much lower and reach values below 10^{-3}. Due to the reduced density in the proximity to the planet the torques are reduced and migration is slowed down.

In a simple picture of type II migration the planet is repelled by both the inner and the outer gap edge because of the same mechanisms resulting in type I migration. This way the planet is locked in the middle of the gap because the repelling force will increase in

case the planet gets closer to one of the edges. If no gas can cross the gap the planet cannot move independently from the gas and its movement is locked to the viscous evolution of the disk (Lin & Papaloizou 1986). In a viscous gas disk the radial speed in equilibrium is fixed by the angular momentum transport to

$$u_r^{\text{visc}} = -\frac{3}{2}\frac{\nu}{r}, \tag{1.8}$$

and if the planet is locked in the gap it will migrate at the same rate as the gas, $\dot{a}_\text{P} = u_r^{\text{visc}}$. As the planet becomes more massive, larger torques are required to move the planet. Because the torques are generated by gravitational forces of the disk, these can no longer be strong enough to move the planet if the disk mass $M_\text{D} \approx 4\pi a_\text{P}^2 \Sigma_\text{P}$ is no longer larger than the mass of the planet, $M_\text{D} \lesssim M_\text{P}$. Because of that, type II migration is often described as (Baruteau et al. 2014)

$$\dot{a}_\text{P} = u_r^{\text{visc}} / \max(1, M_\text{P}/M_\text{D}). \tag{1.9}$$

For a Jupiter mass planet this means it would migrate from 5 au all the way to the star within about 10^5 years which is still fast compared to the lifetime of the disk of ~ 2.5 Myr.

1.5.3 Type III migration

Type III migration is also called runaway migration because it can become extremely fast with migration timescales of 100 orbits or even less. It can occur for planets which are just starting to open a gap but are not yet massive enough to open a full gap.

If a planet is migrating radially inwards there will be gas close to the horseshoe region which will only make a single U-turn which means after just one encounter with the planet it will move from the inner to the outer disk. During the encounter the gas gains angular momentum from the planet so there is a torque acting on the planet

$$\Gamma_\text{Flow} = 2\pi \Sigma_\text{s} \dot{a}_\text{P} \Omega_\text{P} a_\text{P}^3 x_\text{s}, \tag{1.10}$$

where x_s is the half width of the separatrix, the streamline separating the inner or outer disk from the horseshoe region, Σ_s is the surface density at the inner separatrix, a_P is the semi-major axis of the planet and therefore $\dot{a}_\text{P}$ is the migration rate. The migration rate in the torque formula means there is positive feedback which then can lead to a runaway migration.

To fully understand type III migration also the drag of the gas contained in the horseshoe region which strongly depends on the surface density in the annulus close to the planet must be taken into account. Without a gap starting to form, this mass would slow down the migration preventing the rapid migration. To make a difference of course the mass of the gas no longer slowing down the migration must be on the order of the planetary mass which can happen for massive disks and planets of Saturn-mass (Masset & Papaloizou 2003).

1.6 Applications

Understanding the migration of planets is important for many reasons. In most cases where planet migration is modeled there is only one planet in an otherwise empty disk. As we know from observed exoplanets, most planets are part of a planetary system as it is also the case for the Solar System. Because of different and in some cases very long timescales (disk dissipation) and unknown initial conditions it is very challenging to model the formation process of multiple planets at the same time. A way to overcome this problem is by not simulating the whole system in detail but to put together a set of simplified models for each subprocess. These subprocesses can often be simplified, for example the disk evolution can be modeled as 1-dimensional diffusion coupled with a process for disk dissipation. Then Planets are point-like objects which interact with the gas disk by prescriptions depending on the local state of the disk without considering the underlying physical effects. With n-body integration many objects in the same disk can be simulated. This allows to model the behavior of a planetary system from early phases up to the final configuration. This method is called *population synthesis* and is very powerful to get a picture of the whole process of planet formation. Because it is computationally cheap it is feasible to simulate a large ensemble of systems with slight variations and generate a statistical sample. By comparing this to observations the underlying prescriptions can be tested. This is usually not possible for simulations trying to model only one effect in detail.

Of course, for useful results population synthesis models depend crucially on accurate prescriptions of the underlying physical processes. The migration of massive planets is even more important, because the movement of giant planets shapes large regions in the disk and can influence the orbits of dust, planetesimals and terrestrial planets.

An example is our own Solar System. The *Grand Tack scenario* devised by Walsh et al. (2011) is a possible formation scenario specifically developed for the Solar System to explain some observational constrains. The most important points are the low mass of Mars, the amount of water on the inner planets and the location and mass of the asteroid belt between Mars and Jupiter. The idea is that Jupiter during its formation migrated inwards to less than 2 au and thus truncated the inner disk. Then Saturn, migrating faster because of its lower mass, catched up with Jupiter and was captured in a 3:2 mean motion resonance. This is a very stable configuration and thus the planets maintained this ratio of orbital periods. As both planets opened a gap in the disk and they were so close together their gaps merged to a common gap enclosing both Jupiter and Saturn. This common gap with the less massive planet on the outer orbit lead to outward migration because the planets remained in resonance but torques from the inner gap edge pushing the planets outwards are stronger than those from the outer edge as they correspond to the mass of the planet creating this gap edge. When the planets increased their semi-major axes the inner disk was left truncated and thus Mars could not reach a mass comparable to Earth's mass that would be expected at that location. During the inward and the outward migration planetesimals from the inner and outer disk were redistributed. Hence, the ice-rich planetesimals from the outer disk reached the inner disk and could have brought water to the inner Solar System. Because the large region between Mars and Jupiter was left void of larger bodies the asteroid belt could form there. Because the asteroid belt's combined mass is only about $5 \times 10^{-4}\, M_\oplus$ it was not heavy enough to form another planet.

However, it is important to point out that the Grand Tack scenario is a complicated sequence of processes fine-tuned to match the outcome to the Solar System we observe today. It is obvious that to model a very precise outcome the initial conditions must be selected very carefully, but in general a model which was stable against small perturbations of the initial conditions would be favorable.

2 Objectives

The simple model of type II migration described in section 1.5.2 unfortunately has some problems. Most important, it is not clear yet why migration eventually stops and what prevents the planets from falling into the star (Hasegawa & Ida 2013). Observations show that gas planets tend to pile up at $r \gtrsim 1$ au (Fig. 1.3) if hot Jupiters are disregarded because of the detection bias favoring them. The discussed model of type II migration has no inherent mechanism that would stop migration and result in the observed planet distribution. The only way to considerably slow down type II migration is by reducing the mass of the gas disk (see Eq. 1.9) or by reducing the viscosity in Eq. 1.8. As the infrared excess of protoplanetary disks has been measured this allows to estimate the accretion rate through the disk onto the star and thus the viscosity is constrained. The disk density in late protoplanetary disk will decrease due to effects leading to disk dissipation. However, a comparison of the important timescales, the disk lifetime of about 2.5 Myr and the type II migration timescale of about 0.1 Myr, indicates that very precise timing of rapid disk dissipation and planet migration would be needed to reach the observed planet population. Hence it is clear, that type II migration as it is currently understood cannot be the full picture.

Already Edgar (2007) found that type II migration is not identical to the viscous inflow rate and the work of Duffell et al. (2014) also showed type II migration behaves differently compared to the classical models. The work by Hasegawa & Ida (2013) discusses among other effects how gas flow across the gap could prevent type II migration to result in giant planets being lost by migration into the star. Together with the general problem of type II migration mentioned above this was the motivation to further investigate how massive planets migrate after they formed a gap and how the radial flow of gas depends on the migration rate.

There are only very few studies actually simulating giant planet migration and most numerical models of type II migration did not capture all properties of the disk that are essential. The radial inflow of gas due to the viscosity in the disk was usually not modeled and because the natural migration rate of type II migration is identical with the radial

inflow speed a complete model should include this effect. Thus, the main objective for this thesis was to create a more complete model of massive planet migration in the type II regime and to analyze which are the important differences to the assumptions made in classical type II migration theory. To do this the well tested code NIRVANA, originally developed by Ziegler & Yorke (1997) and extended over the years by Gennaro D'Angelo and Bertram Bitsch among others, was adopted. For the models in this project some further improvements were needed. The most important part added was the ability to model an equilibrium accretion disk with the correct radial gas speed as in Eq. 1.8 and thus simulate a disk with an accretion flow through the disk and onto the star. This way the disk model is much more realistic and it contains the important ingredients needed for type II migration.

The first step was to model type II migration and analyze the migration rates for a wide range of parameters and check these against the established model of type II migration. As we found similar deviations as Edgar (2007) and Duffell et al. (2014) we wanted to better understand where the actual migration differs from type II migration.

This meant to delve into three different questions:

- Is the gap really a separation for the inner and outer disk or can gas flow across?
- Is the migration driven by viscosity and where do the torques acting on the planet originate?
- Does accretion onto the planet alter the migration?

The first question is very important as the separation of the disk is a fundamental assumption for type II migration. If gas could flow across the gap (without it all being accreted) the repelling force of the gap edged would not grow until the planet migrated inwards with the same rate as the gas drifts. The second question aims at the strength of the torques acting on the planet. If the torques are just a result of the inward gas drift this should show in the torque density that relates to where the torques are generated. This also includes to measure how the torque changes while the planet is migrating in the disk as this could hint to whether the torques are adjusting to reach a certain migration rate. The last question is related to the first question because a possible flow across the gap is very likely to be affected by the accretion of gas onto the planet. It is also interesting to investigate whether the accretion itself, as it changes the properties of the planet and the gap, could slow down the migration. Also, the question how fast a planet inside a gap is able to grow might have important implications as a very heavy

planet might exceed the local disk mass and migration could stop not because the disk has dissipated but the planet has grown.

All these open questions have to be answered to reach a better understanding of the migration of massive planets. Because massive planets are able to shape a planetary system knowing their migrational behavior is indispensable to understand planet formation in general. Although giant gas planets are not considered to be able to harbor life their effect on much smaller terrestrial planets might be fundamentally important.

3 Publications

Dürmann, C. & Kley, W. (2015). Migration of massive planets in accreting disks. *Astronomy & Astrophysics, 574*, A52

Dürmann, C. & Kley, W. (2016). The accretion of migrating planets. *Astronomy & Astrophysics*, in press, DOI 10.1051/0004-6361/201629074

Statement of own contributions

Both publications were prepared together with my supervisor Prof. Dr. Wilhelm Kley. All published data was generated and analyzed by me and discussed together with Prof. Kley. In the first publication, most writing ($\sim$ 90 %) was done by me except in the introduction and conclusions sections. The introduction was mostly written by Prof. Kley ($\sim$ 70 %) and the conclusions to about equal parts by both of us (each $\sim$ 50 %). The second paper was mostly written by myself ($\sim$ 90 %).

A&A 574, A52 (2015)
DOI: 10.1051/0004-6361/201424837

Astronomy & Astrophysics

Migration of massive planets in accreting disks

C. Dürmann and W. Kley

Institute of Astronomy and Astrophysics, Universität Tübingen, Auf der Morgenstelle 10, 72076 Tübingen, Germany
e-mail: christoph.duermann@uni-tuebingen.de

Received 20 August 2014 / Accepted 3 December 2014

ABSTRACT

Aims. Massive planets that open a gap in the accretion disk are believed to migrate with exactly the viscous speed of the disk, a regime termed type II migration. Population synthesis models indicate that standard type II migration is too rapid to be in agreement with the observations. We study the migration of massive planets between 2×10^{-4} and 2×10^{-3} $M_\odot$, corresponding to 0.2 to 2 Jupiter masses M_J to estimate the migration rate in comparison to type II migration.
Methods. We follow the evolution of planets embedded in two-dimensional, locally isothermal disks with non-zero mass accretion, which is explicitly modelled using suitable in- and outflow boundary conditions to ensure a specific accretion rate. After a certain relaxation time we release the planet and measure its migration through the disk and the dependence on parameters, such as viscosity, accretion rate, and planet mass. We study accreting and non-accretion planets.
Results. The inferred migration rate of the planet is determined entirely by the disk torques acting on it and is completely independent of the viscous inflow velocity, so there is no classical type II migration regime. Depending on the local disk mass, the migration rate can be faster or slower than type II migration. From the torques and the accretion rate profile in the disk we see that the gap formed by the planet does not separate the inner from the outer disk as necessary for type II migration, rather gas crosses the gap or is accreted onto the planet.

Key words. protoplanetary disks – planet-disk interactions

1. Introduction

The interaction of the growing protoplanet with the ambient disk leads to a change in the orbital elements of the planet. The most important for the overall evolution of the planet is the change in semi-major axis, i.e. the migration of the planet. The topic of planet-disk interaction and the orbital evolution of planets has been covered in a few recent reviews (Kley & Nelson 2012; Baruteau & Masset 2013; Baruteau et al. 2013), and here we present only a brief summary of the relevant issues. Depending on the mass of the planet, different regimes of migration are distinguished. Most important are the two limiting regimes of types I and II migration.

Type I migration occurs for low mass planets (with a mass less than about 50 $M_\oplus$) that do not open a gap in the disk, and can be treated in the linear regime. Here the total torque is given by the effects of the spiral density waves (Lindblad torques) and the corotation torques generated by the gas flow in the coorbital horseshoe region. In contrast to the Lindblad torque that quite generally leads to inward migration (Ward 1997), the corotation torque suffers from saturation effects making it strongly dependent on on the magnitude of viscosity and thermal diffusion. These can significantly alter the migration speed and may even reverse the direction of the migration. Analytical formulae to account for these effects have been presented by Paardekooper et al. (2010) for adiabatic disks and Paardekooper et al. (2011) for disks with thermal diffusion.

Type II migration occurs for massive planets with masses comparable to M_J or larger. Because of angular momentum deposition in the disk, those planets open an annular gap in the protoplanetary disk at the location of the planet where the density is significantly reduced. In this case the migration speed is slowed down from the linear rate because of the reduced mass available near the planet. During the migration process the gap created by the planet will have to move with the planet through the disk. Hence, it is often assumed that in an equilibrium situation the gap moves exactly with the viscous accretion velocity of the disk, and that the planet is locked in the middle of the gap to maintain torque equilibrium (Ward 1982, 1997; Lin & Papaloizou 1986).

Direct numerical simulations of planet-disk interaction typically place the planet in a non-accreting disk and keep the planet at a fixed position to analyse the torque density distribution from which the migration speed can then be calculated, see Kley & Nelson (2012) for references. Calculations, where gap-opening Jupiter-type planets were allowed to move through the disk as given by the torques acting on them, have been performed for isothermal disks by Nelson et al. (2000) for two-dimensional (2D) simulations. They studied non-accreting and accreting planets where mass from inside the planet's Roche lobe was added to the planet mass. Both cases lead to similar results indicating that a massive planet could migrate within 10^5 years from about 5 au all the way to the center. In full 3D radiative simulations even faster migration rates were found, though only for planets with a maximum mass of about 0.6 M_J (Bitsch & Kley 2010). Numerical calculations of migrating massive planets were carried out by Edgar (2007, 2008). Using a constant kinematic viscosity he came to the result that there is no constant migration rate as predicted for the type II regime. In a related study Paardekooper (2014) analyzed the influence of planetary motion on the type I migration regime. He found that in non-isothermal disks the regime of outward migration can be larger than that estimated for fixed planets.

The migration of massive planets in evolving disks has been analysed by Crida & Morbidelli (2007) for 2D isothermal disks. In their models, the planets were placed in a disk with an initial

Gaussian profile that evolves under a constant kinematic viscosity. Their results show that only planets that carve a deep gap in the disk experience genuine type II migration and move with the viscous speed of the disk. This is the case either for very massive planets or low viscosity disks, with a Reynolds number larger than about 5×10^5. In the case of only partial cleared gaps, i.e. for less massive planets and larger viscosity, they found a reduced migration speed and in some cases even outwards migration, an effect due to the very effective action of the corotation torques. In addition, because of the positive density slope at the location of the planet in their simulations, the Lindblad torques are strongly reduced, which strengthens the effect.

Following this global study there have been recent models of planets embedded in disks with a given (constant) mass accretion rate. Bitsch et al. (2014) focussed on the regime of earth-mass planets in an irradiated accretion disk with a given $\dot{M}$ rate to determine the regimes of inward and outward migration. They modelled axisymmetric disks with vertical structure and used the formula by Paardekooper et al. (2011) to determine the migration properties of the embedded planets. Fung et al. (2014) investigated the structure of gaps created by stationary planet in an accreting disk, but they did not include planet migration. In their 2D isothermal studies they showed that despite the presence of a massive, gap opening planet, which was not allowed to accrete any material, the disks reached an equilibrium state with a constant mass accretion rate. Obviously, in this configuration the mass flow across the gap equals exactly the imposed disk accretion rate, $\dot{m}$. The timescale of type II migration was analysed with respect to the agreement with the orbital properties of the observed massive extrasolar planets by Hasegawa & Ida (2013). They argued that standard type II migration is too rapid and mechanisms need to be found to slow it down.

Recently, Duffell et al. (2014) looked at the migration of planets in accretion disks using an alternative, different approach. Instead of moving the planet according to the disk torques, they pulled a Jupiter mass planet through a zero $\dot{m}$ non-accreting disk, measured the torques acting on the planet, and compared the resulting migration rate with the actual pull rate of the planet. In this way they obtained possible equilibrium solutions of the migration speed of a planet through a disk. In particular, they found that the possible equilibrium migration speed of the planet is independent of the viscous speed and can be lower and smaller than type II migration, depending on the local surface density of the disk.

Hence, it appears that the issue of type II migration is presently not resolved. Theoretically, it is clear that a planet can only be moved by the disk torques acting on it. On the other hand, disk material moves under the action of viscous torques and its local inflow speed is directly proportional to the viscous torque. If a planet migrated exactly in the type II regime, then the disk torque and viscous torque should be equal. In this paper, we make a new attempt at the problem of type II migration and study the migration of planets in 2D isothermal disks with a constant mass accretion rate. In a first step, we construct constant $\dot{m}$ disks with stationary planets of different masses and then, in a second step, we move the planets according to the torques acting on it, measure their migration rate, and compare it to the type II migration rate.

Our setup is described in Sects. 2, and 3 we present our results for fixed planets in accreting disks. In Sect. 4 we move the planets according to the torques acting on them, and compare this in detail to type II migration in Sect. 5. The results are discussed in the final Sect. 6.

Table 1. Parameter space used in our calculations.

α	$\dot{m}$	q
	2×10^{-9}	
	5×10^{-9}	
	1×10^{-8}	
	2×10^{-8}	0.0002
0.001	5×10^{-8}	0.0005
0.003	1×10^{-7}	0.001
0.01	2×10^{-7}	0.002

Notes. The highlighted values define our standard model. In the standard-resolution (251×583) models only one parameter was varied while the other two were constant. In the low-resolution models (135×405) the whole parameter space with $\dot{m} > 10^{-8}$ was covered. The values of α and $q = M_\mathrm{p}/M_\odot$ are dimensionless and $\dot{m}$ is given in $M_\odot$/yr in the whole article.

2. Setup

To study the migration of planets in disks, we assume that the disk is geometrically thin and simplify to a two-dimensional (2D) approximation. The disk is assumed to be locally isothermal and driven by an α-type viscosity. In addition we model explicit mass accretion through the disk. For our calculations we use the NIRVANA-code (Ziegler & Yorke 1997; Ziegler 1998) in a 2D setup. The star is located at the centre of a cylindrical coordinate system, which covers a radial range of 1.56 to 15.6 au corresponding to $r = 0.3 \ldots 3.0$ in code units where the unit of length is given by $r_0 = 5.2$ au. In the following we will specify distances in code units unless specified otherwise. In the azimuthal direction we cover a complete annulus from 0 to 2π. In our standard resolution the domain is covered by 251×583 cells. The planet is placed on a circular orbit at a distance of 5.2 au corresponding to $r = 1.0$.

To speed up the initial relaxation we, first calculated the equilibrium of the disk, without the planet, with a reduced resolution of $(N_r, N_\phi) = (101, 233)$. After 10^6 time steps, corresponding to about 5000 orbits, these results were interpolated to our standard-resolution grid. Then the model could adapt to this new resolution for additional 10^5 time steps (about 290 orbits) before the planet was released. The planet then could move freely in the disk, and change its semi-major axis and eccentricity. In addition, we performed another set of similar calculations with a lower resolution of $(N_r, N_\phi) = (135, 405)$ and extending from $r = 0.2$ to 2.0. Both calculations give similar results, after 1000 orbits the positions of the planets differ by around 5%.

For our studies we varied the viscosity by changing the α-parameter, the accretion rate (and thus the disk surface density, see Eq. (4) below), and the planetary mass. The used parameter space with the highlighted standard model, is shown in Table 1. We limit our planet mass to a maximum of 2 M_Jup (or $q = 0.002$) because for larger m_p the outer disk becomes eccentric (Kley & Dirksen 2006) and migration properties change (D'Angelo et al. 2006).

2.1. Initial and boundary conditions

The goal of this work was to set up a disk with a steady accretion flow through the disk. Hence, matter has to be fed into the domain at the other boundary of the disk (at r_max), transported to the inner disk, leaving the domain at r_min. The local accretion rate through a disk is given by

$$\dot{m} = -2\pi r \Sigma u_r. \quad (1)$$

It depends on the surface density, Σ, and the radial velocity u_r, of the gas. In equilibrium for a constant $\dot{m}$ the viscous accretion velocity is given by

$$u_r^{\rm visc} = -\frac{3}{2}\frac{\nu}{r}, \tag{2}$$

where ν is the kinematic viscosity and r the radial distance to the central star. This result can be obtained for stationary accretion disks with constant accretion rate, derivations can be found in textbooks such as Frank et al. (1992) or Armitage (2010). In our case of an isothermal disk, we use the α-viscosity prescription, $\nu = \alpha c_s H$, (Shakura & Sunyaev 1973) with the disk scale height $H = hr$, where the relative disk thickness is constant, $h = 0.05$. With the isothermal sound speed, $c_s = H\Omega_K$, this can be written as

$$u_r^{\rm visc} = -\frac{3}{2}\frac{\alpha c_s H}{r} = -\frac{3}{2}\alpha h^2 r\Omega_K, \tag{3}$$

where $\Omega_K = \sqrt{GM_*/r^3}$ is the Keplerian orbital frequency with the stellar mass M_* and the gravitational constant G. With given $\dot{m}$ and α this leads in equilibrium to the surface density

$$\Sigma = \frac{1}{3\pi}\frac{\dot{m}}{\alpha h^2 r^2 \Omega_K} = \frac{\dot{m}}{3\pi\alpha h^2\sqrt{GM}}\, r^{-1/2} = \Sigma_0 r^{-1/2}. \tag{4}$$

From radial equilibrium (pressure gradient balanced by centrifugal force and gravity) the angular velocity is given by

$$u_\phi = \sqrt{1 - \frac{h^2}{4}}\, r\Omega_K. \tag{5}$$

Thus, for our initial conditions we use $u_r^{\rm visc}$ from Eq. (3), Σ from Eq. (4) and u_ϕ from Eq. (5), with prescribed values of $\dot{m}$, α and h.

At the outer boundary gas enters the computational domain with $u_r^{\rm visc}$, and Σ_0 is fixed according to the chosen $\dot{m}$. For the standard model with $\alpha = 0.003$ and $\dot{m} = 10^{-7}\ M_\odot/{\rm yr}$, the initial disk density at $r = 1$ is $\Sigma_0 = 878\ {\rm g\,cm^{-3}}$. At the inner boundary only the radial velocity is fixed according to Eq. (3), material then flows out with the local density at $r_{\rm min}$. The azimuthal velocity u_ϕ is held fixed, according to Eq. (5), at both the inner and the outer boundary. In the azimuthal direction, we enforce periodic boundaries. For the gravitational potential, we use ϵ-smoothing with $\epsilon = 0.6H$ (Müller et al. 2012). To prevent density fluctuations due to wave reflection at the radial boundaries the radial and azimuthal velocity is damped towards its azimuthal mean value near the boundaries on a timescale of $\tau_{\rm damp} \approx \Omega_K^{-1}$ with Ω_K taken at the inner and outer boundaries.

2.2. Accretion onto the planet

To study the influence of mass accretion by the planet on the migration speed, we performed additional simulations in the two extreme cases of non-accreting planets and maximally accreting planets. Both cases are of course unrealistic, but reality lies somewhere in between. To model maximal accretion, we implemented the accretion scheme devised by Kley (1999) where at each time step the gas density inside the Roche Lobe $R_R \approx a(q/3)^{1/3}$ of the planet is reduced by a factor of $1 - f_{\rm red}\Delta t$ with $f_{\rm red} = 1/2$. In our simulations, the mass removed in this way is not added to the planet mass.

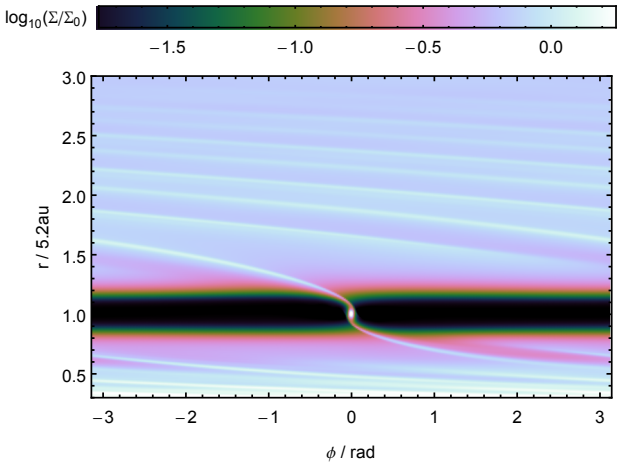

Fig. 1. Surface density of a fixed-orbit, non-accreting planet calculation for the standard model with $(\alpha, M_p/M_*, \dot{m}) = (0.003, 0.001, 10^{-7})$ after 2500 orbits. The planet is in the middle of a stable gap and the accumulation of mass near the planet is clearly visible. The spiral arms are damped at the inner and outer boundary so no reflections are seen.

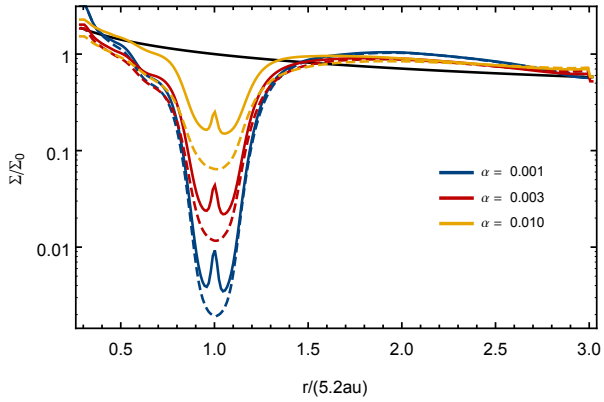

Fig. 2. Azimuthally averaged surface density for a non-accreting (solid line) and an accreting (dashed line) planet with $q = 0.001$, for different values of the viscosity parameter α. The black line indicates the initial density profile at the beginning of the simulation. The red line corresponds to the standard model.

3. The disk structure for fixed planets

Before starting the calculations with moving planets, we constructed equilibrium cases where the planets are not allowed to move and remain at their initial locations. This allows us to estimate the size and depth of a gap as a function of planet mass and the viscosity. The surface density of this calculation for the standard model after 2500 orbits is shown in Fig. 1. There is a very steady gap edge and stable spiral arms resulting from the perturbation of the planet.

The azimuthally averaged surface density in the case of stationary planets is shown for different values of α (in Fig. 2) and q (in Fig. 3). As expected, the gaps are deeper for lower viscosity and higher planet mass. While a more massive planet causes a much wider gap, decreasing the viscosity primarily deepens the gap. In isothermal disks, for stationary planets, the surface density distribution is identical for different values of the accretion rate, and hence $\dot{m}$ has no influence on the gap profiles that are

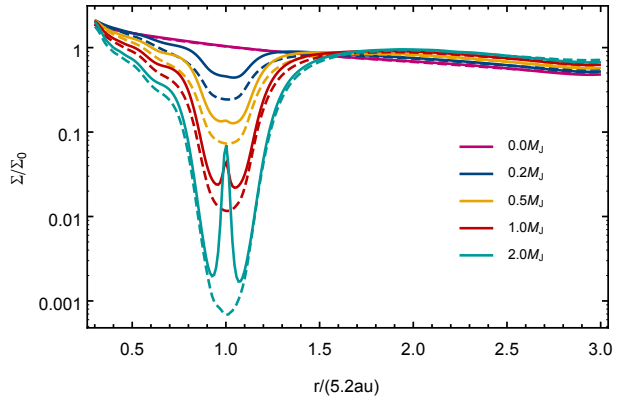

Fig. 3. Azimuthally averaged surface density for non-accreting (solid line) and accreting (dashed line) planets and $\alpha = 0.003$, for different values of the planet mass. The red line corresponds to the standard model.

therefore identical. The gap depth depends on the accretion onto the planet. For non-accreting planets the gap has a clearly visible density bump at the position of the planet. If accretion onto the planet is allowed, the bump disappears and the gap becomes deeper because gas is accreted onto the planet and removed from the simulations.

In the outer disk region, for $r > 1.7$, the surface density is increased over the case without a planet and the amount increases with planet mass. This is because the gas initially in the gap is pushed to the inner and outer regions of the disk, because of angular momentum transfer to the disk. Because, in the outer disk, the gas cannot leave the computational domain the surface density must be increased, the effect being stronger for more massive planets with a deeper gap. Hence, there occurs a jump in the surface density at the outer boundary. This is also clearly seen in Fig. 4 where no logarithmic scale is used. This jump in Σ at $r_{\max}$ has no influence on our results on the migration properties and it disappears if larger $r_{\max}$ are used.

The evolution towards the equilibrium state is shown in Fig. 4 where the radial dependence of the surface density and local accretion rate, $\dot{m}(r)$, are displayed at different times. The migration rate is obtained by integrating the mass fluxes in the advection routine of the code over the ϕ-direction yielding a radial profile of accretion. This ensures consistency with the numerical calculations. In the bottom panel, it is clearly visible that the equilibrium is not yet reached after 3600 orbits. This is because the accretion rate is extremely sensitive to all kinds of perturbations. The equilibrium viscous inflow speed is given by $u_r/c_s \approx \alpha h$, which is about 10^{-4} for our standard model. Hence even small pressure perturbations lead to large variations in the radial velocity, compared to the viscous speed. Thus, although the accretion rate profile is not flat, the changes in the surface density after 2700 and 3600 orbits are very small, and the gap is already fully developed. Obviously, in a steady-state solution the gas must be able to cross the gap. The inner and outer disk are connected and there is no significant pile up at the outer gap edge or depletion at the inner gap edge.

3.1. The torque acting on the planet

To estimate the expected migration rate of planets in disks with mass flow, we calculate the torques generated by the density perturbations in the disk as induced by the planet. In Fig. 5 we

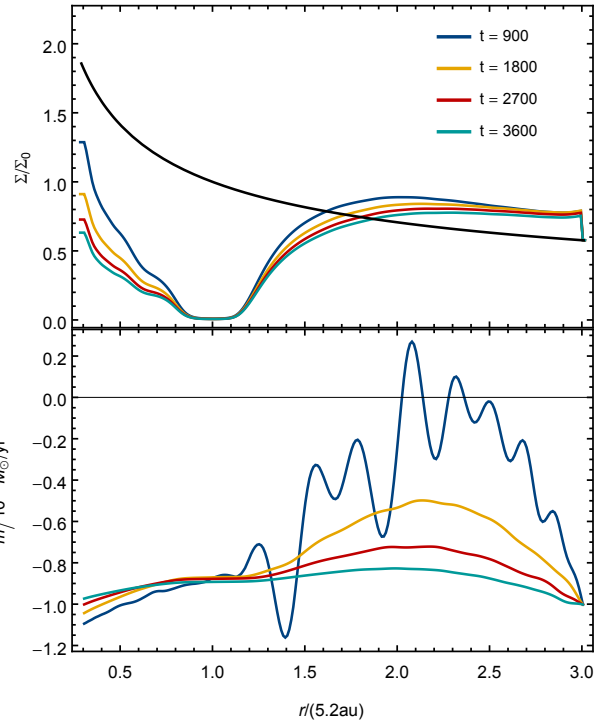

Fig. 4. Azimuthally averaged surface density profile (*top*) and the migration rate profile (*bottom*) in case of $(\alpha, q, \dot{m}) = (0.003, 0.001, 10^{-7})$ as in Fig. 1. The planet is at $r = 1.0$. The profiles are taken at different times after the beginning of the calculation. The black line indicates the initial density profile at the beginning of the simulation before the planet was added.

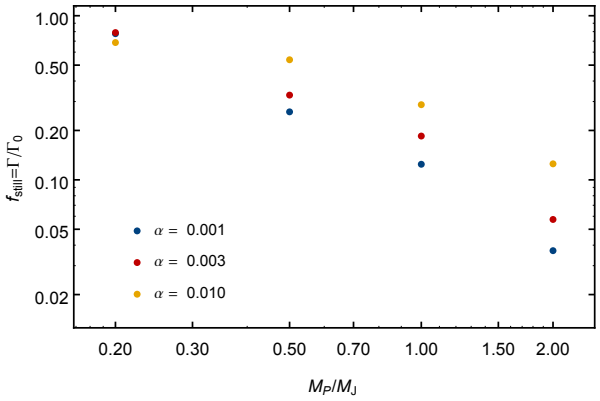

Fig. 5. Normalized torques acting on planet with fixed orbits at the end of the relaxation as a function of the planet mass. The data is taken from the low-resolution calculations. For isothermal disks the normalized torques are independent of the disk density.

display the obtained torques as a function of planet mass M_P for different value of the viscosity. Here, we used the standard torque normalization (see e.g. Paardekooper et al. 2010)

$$\Gamma_0 = -\Sigma_p \Omega_K^2 a_p^4 \left(\frac{q}{h}\right)^2, \tag{6}$$

where Σ_p is the unperturbed surface density at the location of the planet and a_p its semi-major axis. This definition of Γ_0 takes the

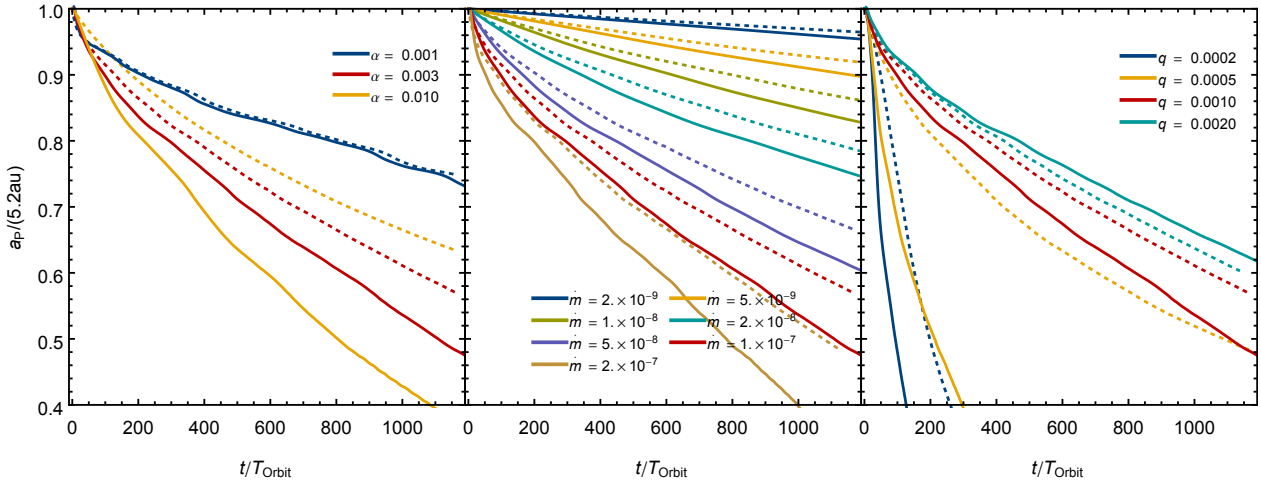

Fig. 6. Planet migration tracks for different model parameter. Starting from the standard model (in red) with $(\alpha, \dot{m}, q) = (0.003, 10^{-7}, 0.001)$, individual parameters have been varied while keeping two others fixed. We varied α (*left panel*), $\dot{m}$ (*middle panel*), and q (*right panel*). The full and dotted lines correspond to non-accreting and accreting planets, respectively.

linear results into account for low mass planets that are subject to type I migration with $\Gamma \propto M_p^2$, massive planets open gaps in the disk that reduce the torque, and a different scaling is expected.

To strengthen the point that these torques are measured for fixed planets that are not allowed to migrate, we introduce the correction factor f_{still} and write for the torque acting on the planet

$$\Gamma = f_{still}\,\Gamma_0. \tag{7}$$

As seen from Fig. 5, the total torque is indeed reduced for larger planet masses. For small planet masses, a flattening is expected as one approaches the type I regime. In our case, the planet masses are still too high, but this effect becomes marginally visible for the higher viscosity models, as expected. On the other hand, there is no visible dependence on variations in the disk mass or the accretion rate (which are coupled here), because in isothermal disks the disk mass is just a scaling factor that depends linearly on the specified $\dot{m}$ value.

4. Migrating planets

After having analysed the equilibrium state for fixed planets, we release now the planets and evolve their orbital elements according to the action of the disk. We measured the migration tracks for many different parameters (see Table 1) for more than 1000 orbits for accreting and non-accreting planets. The migration tracks are shown in Fig. 6 for a variety of model parameters. All planets migrate inwards at a rate that decreases with time. At the beginning of the migration, shortly after the release of the planet, there is a short phase of rapid inward migration that then slows down. This transient phenomenon is caused by the unavoidable small mismatch of a disk structure with a stationary planet in comparison to the evolving case.

In cases where $M_P \lesssim M_D = \Sigma_P a_P^2$, with Σ_P being the undisturbed surface density at the position of the planet a_P, there is no slowing down, rather we observe very fast type III migration, such as for $q \leq 0.0005$ (yellow and blue curve) in the right panel of Fig. 6. Type III migration sets in later for accreting planets.

4.1. Mass accretion onto the planet

Our implementation of the mass accretion onto the planet is very simple, and, therefore, we only used this method to obtain an idea what changes are expected in case of an accreting planet. Because the algorithm takes away the gas near the planet at a high rate, it serves as an upper limit of the possible accretion onto the planet. We found that the general behaviour of accreting planets is similar to the non-accreting cases. As seen in Fig. 6 accreting planets migrate more slowly in most cases. The reason is the reduced density in the vicinity of the planet, which leads to weaker torques. Although the contribution of the planet envelope inside 0.8 Hill-Radii is not considered when calculating the torque (see Crida et al. 2008), the region affected by the accretion is much bigger and thus important for the torques. This effect of accretion is similar to what has been seen in Nelson et al. (2000) who added the accreted material to the dynamical mass of the planet, however. This will lead to an even slower migration of the planet due to the increased inertia.

4.2. Gap profiles during the evolution

The gap profile has an important impact on the migration of a planet. Because the disk is depleted near the planet's orbit, these regions cannot contribute to the torques on the planet. In Fig. 7, the change in global disk density is displayed for four different snapshots during the evolution of the planet in our standard model. At the inner edge of the gap, we observe a density pile up that initially increases with the planet moving inwards closer to the inner edge. But when the planet reaches $r \approx 0.7$ at $t = 530$, it decreases again because the gap approaches r_{min}, and at the inner boundary an outflow condition with a given radial velocity is enforced. At the outer gap edge we see the gas lagging behind the movement of the gap. The gap moves $\Delta r = 0.3$ in 530 orbits. The viscous timescale $\tau_{visc} = \Delta r^2/\nu$ for the gas to cover this distance is about 2070 orbits. It is therefore obvious that the planet and the gap move faster than the viscous speed of the gas, which demonstrates that the gap must be dynamically created during the planet's inward motion. The inward motion of the planet and the gap can only be maintained because gas can cross the gap faster than the viscous timescale.

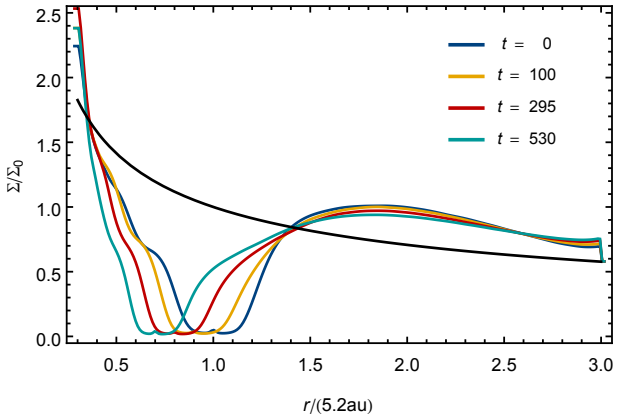

Fig. 7. Global gap profiles at four different times during migration of the planet for the standard model with $q = 0.001$ and $\dot{m} = 10^{-7}$. The black line indicates the unperturbed density profile without the planet.

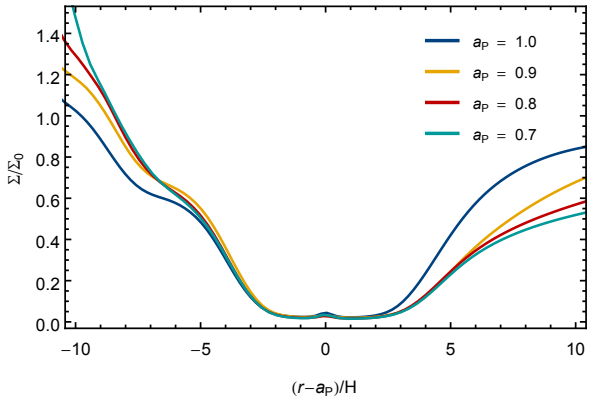

Fig. 8. Gap profiles for the standard model taken at different positions of the planet in the disk during its migration path. The gap is rescaled using the local disk scale height, H, at the position of the planet. The curves correspond directly to those shown in Fig. 7.

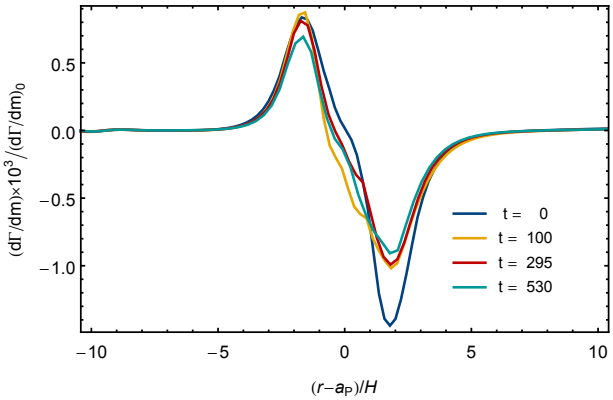

Fig. 9. Specific torques for the same model as in Fig. 8 at the same times and respective positions.

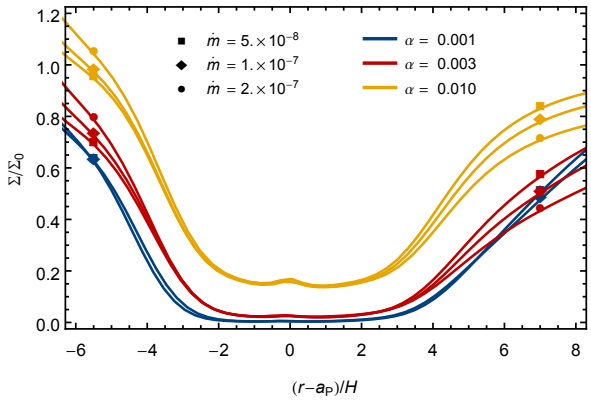

Fig. 10. Gaps of a $q = 0.001$ planet with different accretion rates 100 orbits after the release of its orbit. The gap is rescaled according to the disk scale height at the position of the planet, which varies for different values of α and $\dot{m}$. The gap profiles are taken from the low-resolution calculations.

To obtain a more detailed view on the local disk structure in the gap region, we display in Fig. 8 the gap at different times during the evolution of the planet in the disk. The gap does not change significantly during the migration through the disk if the width is rescaled with the local disk scale height $H(a_\mathrm{p})$ at the actual position of the planet. Farther away from the planet the surface density varies because of the different positions in the disk.

In Fig. 9 the specific torques are displayed where we use the normalization of D'Angelo & Lubow (2010),

$$\left(\frac{\mathrm{d}\Gamma}{\mathrm{d}m}\right)_0 = q^2 h^{-4} a_\mathrm{P}^2 \Omega_\mathrm{P}^2. \quad (8)$$

The biggest contribution is generated within a $5H$ wide region inside and outside the planet. Apart from the initial adjustment of the gap to the moving planet (see Fig. 8) the specific torques reach an equilibrium profile after 100 orbits. As expected from very similar local gap profiles (in Fig. 8), the specific torques do not depend strongly on the position of the planet in the disk. This will be of importance later in explaining the overall migration properties of the planets (see Sect. 5).

As shown in Fig. 10 the gaps, of course, depend on the viscosity. For a fixed α-value, the gap structure near the planet does not change very much, even for different disk masses. Effects farther away from the planet $\gtrsim 4H$ are results from the different positions in the disk as well as the movement of the gap through the disk with different velocities (see Fig. 6). At the inner gap edge the surface density is increased for the higher accretion rates and at the outer gap edge for the smaller accretion rate. This is because the inward migration rate of the planet is faster for a denser disk (and thus a higher accretion rate, see Fig. 6) and the gap edges cannot follow as fast as the planet moves. A higher migration rate therefore leads to a stronger gap deformation. The gap depth depends on α in the same manner as for the static planets in Fig. 2.

4.3. Flow across the gap

Above we have argued that the fast migration speed of the planet implies that mass has to cross the gap. Now we analyse this process in more detail. In Fig. 11 we display the local mass accretion rate through the disk, $\dot{m}(r)$, similar to Fig. 4, but now for a migrating planet at different times after the release. At early times, when the planet is moving inwards very fast, the gas is flowing outwards instead of inwards. Even at later times, when the migration rate has slowed down, at the position of the planet the

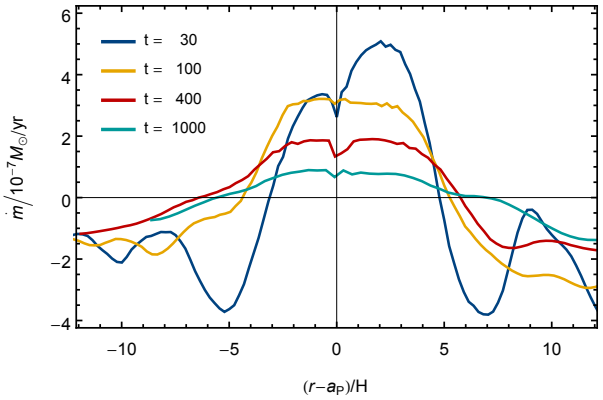

Fig. 11. Azimuthally averaged local accretion rate, $\dot{m}(r)$, at different times during the inward migration of the planet for the standard model ($q = 0.001$, $\dot{m} = 10^{-7}$, $\alpha = 0.003$). The plot is similar to Fig. 4, which has the same parameters, but now for moving planets. To compare the accretion rate near the planet the position is rescaled to units of the disk scale height at the position of the planet. The labels refer to the elapsed time (in initial orbits) after the release of the planet.

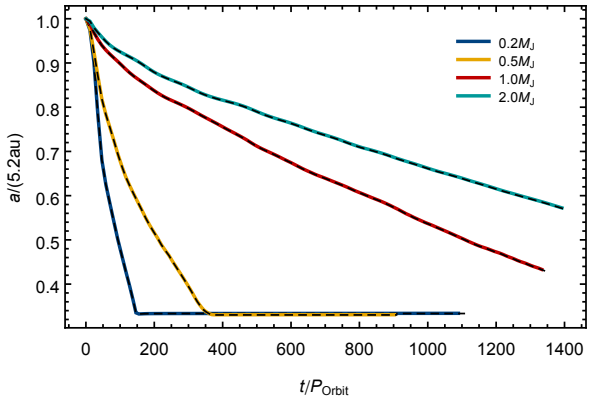

Fig. 12. Migration tracks of planets embedded in disks for different planet masses, for given viscosity and disk accretion rate $(\alpha, \dot{m}) = (0.003, 10^{-7})$. Coloured lines: theoretical tracks calculated by integrating the measured torques. The dashed black lines are the corresponding observed migration tracks in the simulations.

direction of the gas flow is still reversed. This effect is caused by the motion of the planet through the disk, which disturbs the local disk structure and leads locally, at the location of the planet, to a transfer of mass from the inner to the outer disk. The mass transfer is positive because the planet moves faster than the viscous accretion velocity u_r^{visc}. As shown above, the gap is bound to move with the planet, but the planet does not drive the disk structure as whole. In consequence, gas from the inner disk, not able to move inwards faster than u_r^{visc}, has to move outwards, which means crossing the gap in outward direction. For a planet moving more slowly than the viscous speed (for low disk densities) the radial flow remains always negative.

If the disk were separated and gas could not cross the gap, the inner disk would pile up and the region adjacent to the planet in the outer disk would be depleted because the gas could not follow the planet's movement. The more massive inner disk would then yield higher positive torques and slow down or even reverse migration. Thus, seeing transport of the gas outwards is a clear sign that the planet is not bound to the viscous accretion velocity and moves independently.

5. Comparing to type II migration

After having obtained the migration track of planets in disks with net mass flux we are now in a position to compare these to the type II migration speed of a viscously driven disk.

In any case, the migration of a planet can only be driven by the gravitational torques exerted on it by the disk material. To prove this statement, we plot in Fig. 12 the evolution of the planet's semi-major as expected from the calculated total torque, Γ, during its motion through the disk (coloured lines). The migration track $a(t)$ is obtained by integrating the formula

$$\dot{a} = \frac{2\Gamma}{M_\mathrm{p} a_\mathrm{P} \Omega_\mathrm{K}}. \tag{9}$$

As seen in Fig. 12, the observed migration (black dashed lines) agrees perfectly with the calculated migration tracks (coloured lines) throughout the whole simulation. Hence, the migration is indeed completely determined by the torques from the disk, as physically expected.

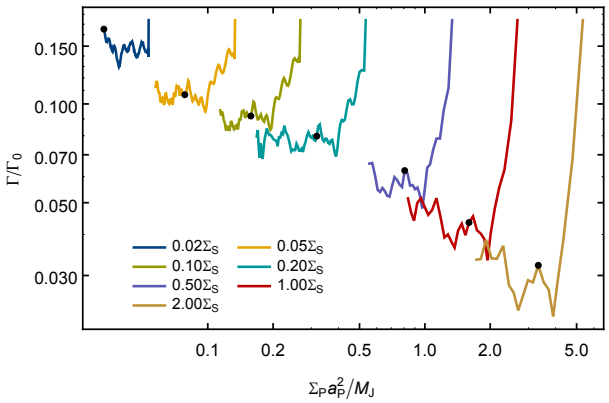

Fig. 13. Normalized torques acting on a Jupiter mass planet as a function of the local disk mass, with $\alpha = 0.003$ and $q = 0.001$. Shown is the evolution of the torques during the migration process, each track starts at the rightmost point with the highest value of $\Sigma_\mathrm{P} a_\mathrm{P}^2$. The black dots mark the point when the planet has reached $a_\mathrm{P} = 0.7$. During the inward migration the local disk mass $\Sigma_\mathrm{P} a_\mathrm{P}^2$, where Σ_P is the surface density in the undisturbed surface density profile at planet position a_p, decreases. The models differ in their initial disk density Σ_0 varied by the disk accretion rate $\dot{m}$, where Σ_S corresponds to $\dot{m} = 10^{-7}$. The torques are averaged over 50 orbits.

Having shown that the torques determine the migration of the planet, we plot in Fig. 13 the normalized torques using the same normalization, Γ_0 as before in Fig. 5. Note that now the normalization factor Γ_0 is a function of the planet's position, see Eq. (6). In Fig. 13 the torques are displayed during the evolution of the planet. The initial location refers to the rightmost points in the individual curves. They all start at the same height $\Gamma/\Gamma_0 = 0.18$ as given by the fixed planet resultis, see Fig. 5. During the inward migration the value of $\Sigma_\mathrm{p} a_\mathrm{p}^2$ decreases. The black dot in each curve corresponds to the time where the planet has reached $a_\mathrm{p} = 0.7$.

Let us first compare the findings to the linear case, for small mass planets that do not open gaps. 2D simulations yield the following relation for the total Lindblad torque on planets (see Tanaka et al. 2002; Paardekooper et al. 2010)

$$\frac{\Gamma_\mathrm{L}}{\Gamma_0} = 3.2 + 1.468\, p, \tag{10}$$

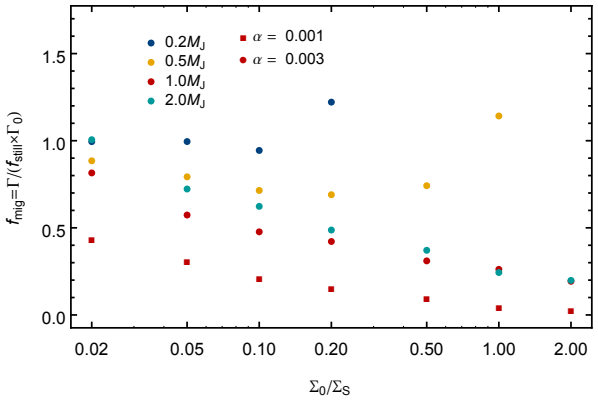

Fig. 14. Slow down factor $f_{\rm mig}$ depending on the disk density for different planetary masses and viscosities. Here, the surface density is given in units of Σ_S, as defined in Fig. 13. The circles are results for $\alpha = 0.003$ and the squares for $\alpha = 0.001$.

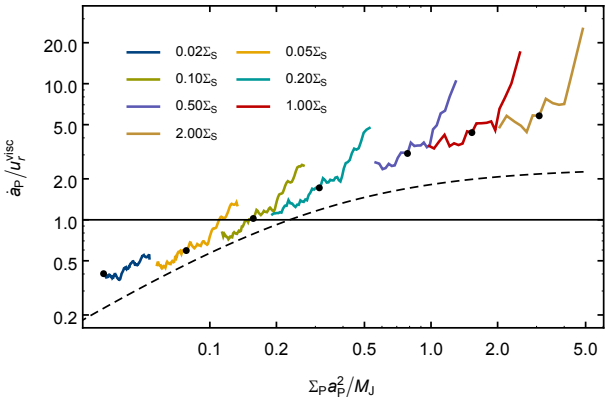

Fig. 15. Migration rate of a Jupiter mass planet normalized by the viscous accretion velocity. Apart from the different y-axis the plot is similar to Fig. 13. The horizontal line corresponds to $u_r^{\rm visc} = 1$. The dashed line shows a fit of Duffell et al. (2014), but they used constant viscosity equal to $\alpha = 0.01$ at $r = 5.2$ au, so their fit is normalized with $u_r^{\rm visc}$ for that α.

where p is the exponent of the surface density profile, with $\Sigma(r) \propto r^{-p}$, and so $p = 0.5$ in our case. This yields $\Gamma_L/\Gamma_0 = 3.934$. Expression (10) was derived for much less massive planets in the regime of type I migration and is not directly applicable to our calculations. The idea is to compare the migration speed of massive planets to the linear type I regime. As shown in Fig. 13 the torques are about 20 to 100 times smaller than the linear results, a consequence of the gap. Additionally, the results show a clear dependence on the density of the disk. In the linear case one would expect a constant ratio Γ/Γ_0 for all disk densities.

This fact is not apparent overall, but after the disk and the gap have adapted to the moving planet, the torques become constant for each individual curve, i.e. for each disk density. This implies that the normalized torques for a given planetary mass and α-value are completely defined by the disk density alone. Therefore, we introduce a slow down factor for migrating planets $f_{\rm mig}$, which gives the factor by which the torques acting on the moving planet are smaller than those for the same planet on a fixed orbit. Because for gap-opening planets the fixed-orbit torques are again smaller by a factor $f_{\rm still}$ than the type I torques Γ_0 (see Fig. 5) we obtain the following expression for the torque of a moving planet

$$\Gamma = f_{\rm mig}\, f_{\rm still}\, \Gamma_0. \tag{11}$$

In Fig. 14 we show the slow down factor $f_{\rm mig}$ for various parameters. For small disk densities the slow down factor decreases with increasing disk density. For light planets with $M_P < M_J$ this changes for Σ_0/Σ_S between 0.1 and 0.5 and the slow down factor strongly increases to values much bigger than one, which marks the onset of type III migration. For the highest disk densities, the slow down factor for the lighter planets are in fact out of the plot range and reach values up to $f_{\rm mig} = 12$. In case of smaller viscosity $f_{\rm mig}$ decreases, but for the same planetary mass the overall structure seems to remain the same.

In Fig. 15 we compare the obtained migration speed to the type II migration rate as given by the viscous inflow speed $u_r^{\rm visc}$. In the case of classical type II migration, the curves should be independent from disk mass and identical to the viscous inflow speed, apart from the adjustment in the beginning. However, the results show a clear dependence with disk mass. Obviously, the actual migration of a planet is not coupled to the viscous evolution in the disk, as also pointed out recently by Duffell et al. (2014). Qualitatively, the relationship between disk mass and migration rate is similar to that found by Duffell et al. (2014) found by different means (see dashed curve in Fig. 15). In our case the inward migration is faster than theirs. For light disks with $\Sigma_D = \Sigma_P a_P^2 < 0.2 M_J$ only, we find that migration becomes smaller than the viscous speed. Here, it is important to note that the viscous speed for our constant $\dot{m}$ models scales directly as $u_r^{\rm visc} \propto a_p\Omega$ the quantity that Duffell et al. (2014) used in their plots.

From our results we obtained for moving planets that the normalized torque Γ/Γ_0 was constant during the evolution of a planet (see Fig. 13). This implies that the torque reduction factors $f_{\rm mig}$ and $f_{\rm still}$ do not depend on the local disk mass, and are only functions of the planet mass and the disk viscosity. Using Eq. (9) for the migration rate and the scaling for Γ_0, we obtain for each planet track

$$\dot{a} \propto a_P^{3/2}\, f_{\rm slow}\, \Sigma_P M_P, \tag{12}$$

where $f_{\rm slow} = f_{\rm mig}\, f_{\rm still}$. Using the relation $u_r^{\rm visc} \propto r^{-1/2}$, as inferred from Eq. (3) for constant H/r, one finds

$$\frac{\dot{a}}{f_{\rm slow} u_r^{\rm visc} M_P} \propto a_P^2 \Sigma_P. \tag{13}$$

This relation is plotted in Fig. 16 and indeed the data lie on a straight line, for all the models with different $\dot{m}$. The data for an accreting planet fall onto the same line. In case of different viscosity there is a shift due to the change in $f_{\rm slow}$, but it follows the same trend.

6. Summary and conclusions

We have studied the migration of massive planets in locally isothermal disks with net mass flow, $\dot{m}$, through them. In our initial step, keeping the planet at a fixed location, we showed that despite the presence of the planet, the disk can nevertheless transport the full $\dot{m}$ through the disk and the gap. We analysed the structure of the gap for different planet masses and viscosities. As expected, the depth of the gap increases with planet mass and is reduced with increasing viscosity. Our gap structure and depths for these models are in very good agreement with the empiric formulae presented in Fung et al. (2014). Additionally,

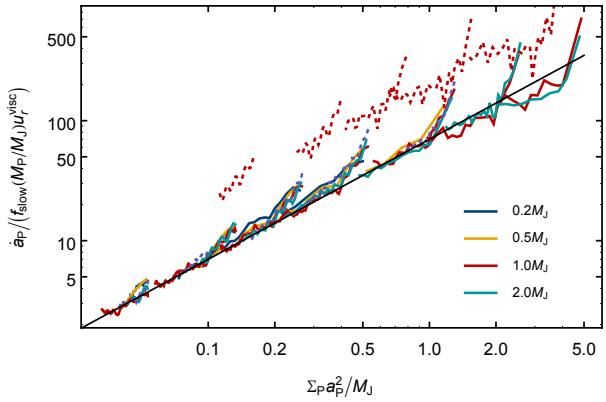

Fig. 16. Normalized migration rates of planets with different masses between 0.2 and 2 M_J. The migration rate is scaled with the slow down factor and planet mass (see Eq. (13)). The slope of the black line is 1. The dotted line corresponds to $\alpha = 0.001$. Accreting planets are indistinguishable from the non-accreting planets and therefore not shown here. Otherwise the plot is similar to Fig. 13.

the gap opening criterion by Crida et al. (2006) gives a suitable condition if there is a considerable gap depth, ≈0.1 of the ambient density. For large planet mass the normalized torque on the planet strongly decreases (see Fig. 5), in contrast to the linear rate where Γ/Γ_0 has no dependence on planet mass. This is a consequence of the increased gap width with a reduced mass that can drive the planet.

Upon releasing the planet we find rapid inward migration, often faster than the typical viscous inward drift of the disk material. As expected, the planet moves exactly according to the disk torques acting on it. A migration independent of the disk's drift speed implies that material can cross the gap region during the migration process. We performed simulations without and with mass accretion onto the planet where, in the latter case, the accretion rate was near the maximum possible rate (Kley 1999). As expected, because of the reduced mass in the vicinity of the planet, the migration rate is reduced below the non-accreting case, but only by about 25%. Our main result is summarized in Fig. 15, which shows that the planet migration does not depend on the viscous inflow speed of the disk material. For small disk masses ($M_D/M_J < 0.2$) only, a Jupiter mass planet moves slower than the disk material. For higher disk masses (given by higher $\dot{m}$ in our calculations), values and subsequently larger surface densities, Σ, the inward migration becomes faster as well.

An important result of our simulations is the finding that during the migration of the planet the normalized torques remain constant, a feature seen by Duffell et al. (2014). In principle, it might be possible to extract approximate analytical relationships for the slow down factors f_{mig} and f_{still}, which would then be useful to calculate theoretical migration tracks to be used, for example, in population synthesis models. To do this, more elaborate parameter studies will be necessary in the future.

Very qualitatively the shape of the curve is similar to that found by Duffell et al. (2014) by a complementary method, but we do not see signs of saturation. Our migration rate is typically faster than theirs up to a factor of 2, but note that their results have been obtained for a spatially constant viscosity, which implies a spatially variable α-value. Because of their special technique of pulling the planet through the disk and measuring the torque after reaching equilibrium, it is not know at which distance of the planet this occurs. Hence, the value of α is not known and the curves cannot directly be compared to each other as the torque depends on the value of α. Edgar (2007, 2008) also used constant viscosity. He also finds that the migration rate depends on the disk mass and the migration timescales are comparable to those we found.

Our findings are also in agreement with those of Nelson et al. (2000) who analysed the migration of a planet in a global disk and constant kinematic viscosity. They inferred a timescale for migration of a massive planet from its starting location at 5 au to 2.5 au of about 2500 orbits, but did not compare this to the viscous accretion rate.

For sufficiently low planetary mass, $M_P \lesssim M_D$, but with M_P still large enough to open a partial gap, the planets can enter the very fast type III migration regime where the migration timescale becomes very short, of the order of about 100 dynamical times. The conditions necessary for type III migration (Masset & Papaloizou 2003) indicate that is may be relevant in the early phases of planet formation with larger disk masses, or in more massive self-gravitating disks.

For low disk masses $M_D/M_J < 0.2$, the migration rate becomes lower than type II migration. These small disk masses occur only during the end phases of the planet formation process when the accretion rate has already reduced significantly.

In this work, we studied only 2D disks and found that disk material can always cross the gap region as required by the migration speed of the planet. For massive, Jupiter type planets the averaged gap profile is identical for 2D and 3D disks (Kley et al. 2001) and one may expect very similar mass flow rates across the gap region, and hence similar migration accretion rates. The additional assumption of locally isothermal disks is not very restrictive as well because for massive planets that do open significant gaps, the dynamical behaviour is very similar to the isothermal case as has been shown by Bitsch & Kley (2010) for full 3D simulations of radiative and isothermal disks.

Nevertheless, it may be interesting to perform in the future 3D simulations of embedded, massive planets in radiative disks and analyse their migration properties. Those simulations are also important to understand better the mass growth of planets because the inclusion of the 3rd dimension may affect the mass accretion onto the planet, while it only mildly affects the migration.

Our results have consequence for population synthesis models in that a modification of the assumed type II migration speed is required for the models, based on the torques acting on the planets. Possibly, more elaborate models that cover a larger parameter space will allow the construction of suitable fit formulae for the migration of massive planets in the future, but this is beyond the scope of the present work.

Another point to consider is the angular momentum balance of the planet. We have taken out mass from the planet's Roche lobe, but have not added this to the planet mass. In addition to the mass, the angular momentum of this material, which is gained by the planet, has to be considered. A fraction of this will change the orbital angular momentum, which will influence the migration of the planet. Future simulations need to consider this effect as well.

Acknowledgements. We thank Bertram Bitsch for very fruitful discussions and acknowledge the constructive and helpful comments from the referee to improve this paper. The calculations were performed on systems of bwGRiD, the computer grid of the Baden Württemberg state. The work of Christoph Dürmann is sponsored with a scholarship of the Cusanuswerk.

References

Armitage, P. J. 2010, Astrophysics of Planet Formation (Cambridge University Press)
Baruteau, C., & Masset, F. 2013, in Lect. Notes Phys. (Berlin: Springer Verlag), 861, 201
Baruteau, C., Crida, A., Paardekooper, S.-J., et al. 2014, in Protostars and Planets VI (University of Arizona Press), eds. H. Beuther, R. Klessen, C. Dullemond, & Th. Henning [arXiv:1312.4293]
Bitsch, B., & Kley, W. 2010, A&A, 523, A30
Bitsch, B., Morbidelli, A., Lega, E., & Crida, A. 2014, A&A, 564, A135
Crida, A., & Morbidelli, A. 2007, MNRAS, 377, 1324
Crida, A., Morbidelli, A., & Masset, F. 2006, Icarus, 181, 587
Crida, A., Sándor, Z., & Kley, W. 2008, A&A, 483, 325
D'Angelo, G., & Lubow, S. H. 2010, ApJ, 724, 730
D'Angelo, G., Lubow, S. H., & Bate, M. R. 2006, ApJ, 652, 1698
Duffell, P. C., Haiman, Z., MacFadyen, A. I., D'Orazio, D. J., & Farris, B. D. 2014, ApJ, 792, L10
Edgar, R. G. 2007, ApJ, 663, 1325
Edgar, R. G. 2008, unpublished [arXiv:0807.0625]
Frank, J., King, A., & Raine, D. 1992, Accretion power in astrophysics (Cambridge University Press)
Fung, J., Shi, J.-M., & Chiang, E. 2014, ApJ, 782, 88
Hasegawa, Y., & Ida, S. 2013, ApJ, 774, 146
Kley, W. 1999, MNRAS, 303, 696
Kley, W., & Dirksen, G. 2006, A&A, 447, 369
Kley, W., & Nelson, R. P. 2012, ARA&A, 50, 211
Kley, W., D'Angelo, G., & Henning, T. 2001, ApJ, 547, 457
Lin, D., & Papaloizou, J. 1986, ApJ, 309, 846
Masset, F. S., & Papaloizou, J. C. B. 2003, ApJ, 588, 494
Müller, T. W. A., Kley, W., & Meru, F. 2012, A&A, 541, A123
Nelson, R. P., Papaloizou, J. C. B., Masset, F., & Kley, W. 2000, MNRAS, 318, 18
Paardekooper, S.-J. 2014, MNRAS, 444, 2031
Paardekooper, S.-J., Baruteau, C., Crida, A., & Kley, W. 2010, MNRAS, 401, 1950
Paardekooper, S.-J., Baruteau, C., & Kley, W. 2011, MNRAS, 410, 293
Shakura, N. I., & Sunyaev, R. A. 1973, A&A, 24, 337
Tanaka, H., Takeuchi, T., & Ward, W. R. 2002, ApJ, 565, 1257
Ward, W. R. 1982, in Lunar and Planetary Science Conference, 13, 831
Ward, W. R. 1997, Icarus, 126, 261
Ziegler, U. 1998, Comp. Phys. Comm., 109, 111
Ziegler, U., & Yorke, H. W. 1997, Comp. Phys. Comm., 101, 54

Astronomy & Astrophysics manuscript no. accretion
November 3, 2016

The accretion of migrating giant planets

Christoph Dürmann and Wilhelm Kley

Institute of Astronomy and Astrophysics, Universität Tübingen, Auf der Morgenstelle 10, 72076 Tübingen, Germany
e-mail: christoph.duermann@uni-tuebingen.de

November 3, 2016

ABSTRACT

Context.
Aims. Most studies concerning the growth and evolution of massive planets focus either on their accretion or their migration only. In this work we study both processes concurrently to investigate how they might mutually affect one another.
Methods. We modeled a two-dimensional disk with a steady accretion flow onto the central star and embedded a Jupiter mass planet at 5.2 au. The disk is locally isothermal and viscosity is modeled using a constant α. The planet is held on a fixed orbit for a few hundred orbits to allow the disk to adapt and carve a gap. After this period, the planet is released and free to move according to the gravitational interaction with the gas disk. The mass accretion onto the planet is modeled by removing a fraction of gas from the inner Hill sphere, and the removed mass and momentum can be added to the planet.
Results. Our results show that a fast migrating planet is able to accrete more gas than a slower migrating planet. Utilizing a tracer fluid we analyzed the origin of the accreted gas originating predominantly from the inner disk for a fast migrating planet. In the case of slower migration, the fraction of gas from the outer disk increases. We also found that even for very high accretion rates, in some cases gas crosses the planetary gap from the inner to the outer disk. Our simulations show that the crossing of gas changes during the migration process as the migration rate slows down. Therefore, classical type II migration where the planet migrates with the viscous drift rate and no gas crosses the gap is no general process but may only occur for special parameters and at a certain time during the orbital evolution of the planet.

Key words. planets and satellites: formation – planets and satellites: gaseous planets – protoplanetary disks – planet-disk interactions – Accretion, accretion disks

1. Introduction

Mass accretion onto giant planets during their growth phase is a delicate process depending on many aspects of the disk structure and a variety of physical processes. One of these is the radial migration of the planet. If the planet is migrating through the disk, important parameters like density, temperature, and viscosity change depending on the migration rate. This has implications on the gap opened by the planet and might eventually alter accretion onto the planet. The simulations carried out for this paper cover global aspects such as planetary gaps and migration in order to study their influence on the accretion process.

The main driving force for the migration of massive planets is the interaction with the surrounding protoplanetary disk. The different migration regimes and the contributing physical effects are discussed in several recent reviews on planet disk interactions by Kley & Nelson (2012), Baruteau & Masset (2013), and Baruteau et al. (2014). The general idea of type II migration was devised by Ward (1982) and Lin & Papaloizou (1986) and states that a planet massive enough ($> 0.5\,M_{\rm Jup}$) will open a gap in the gas disk around the protostar. Under the assumption that the gap follows the viscous evolution and moves inward with the radial viscous speed, and because the gap edge creates torques repelling the planet, it is locked in the middle of the gap and has to follow the viscous disk evolution.

This picture has to be revised after recent findings showing that a planet in a gap usually migrates at rates faster or slower than the viscous rate (Edgar 2007; Morbidelli & Crida 2007; Duffell et al. 2014; Dürmann & Kley 2015). This is important for models of population synthesis because the role of type II migration is not yet clear (Hasegawa & Ida 2013). For classical type II migration it is crucial to have a gap which separates the inner from the outer disk because only in this case is the gap forced to follow the viscous evolution of the gas. If gas can cross the gap this means there are different channels of transportation for the gas and the viscous speed of the gas does not need to coincide with the migration rate of the planet. This cannot be modeled separately from planet migration because for stationary planets in equilibrium there will automatically be a gas flow across the gap matching the disk accretion rate, something also found by Fung et al. (2014). Also, for low-mass planets it has become clear that to study migration, the analysis of static torques is not sufficient. Recent work by Paardekooper (2014) and Pierens & Raymond (2016) showed that dynamical torques resulting from the migration must also be considered.

Giant planet accretion has been investigated by several groups in various ways. One kind of research focuses on the inner structure and the atmosphere of the growing planet (Pollack et al. 1996; Hubickyj et al. 2005). They do not explicitly model the protoplanetary disk around the planet but this way they have a very high resolution of the interior of the planet and its close surroundings. Another kind of simulation models the whole disk and inserts the planet at some stage in its evolution. See Lubow et al. (1999), for example. Because the whole disk, in two-dimensions (2D) or even three-dimensions (3D), has to be modeled, the limiting factor is the resolution in the vicinity of the planet, which can be overcome to some degree by adap-

Article published by EDP Sciences, to be cited as http://dx.doi.org/10.1051/0004-6361/201629074

tive mesh refinement or nested grids, as used by D'Angelo et al. (2003).

In this paper we focus on the mutual effects of the gas accretion and giant planet migration. In particular, we investigate where the accreted gas originates in the disk and study influence of the gap. With respect to type II migration we analyze whether gas can cross the gap and how this is affected by the mass accretion rate onto the planet.

In Sect. 2 the numerical model we used is explained, and in Sect. 3 we describe the method we used to model accretion. In Sect. 4 we discuss the effect of varying the accretion rate and how this affects the migration rate. The effects of different models of accretion are discussed in Sect. 5. In Sect. 6 we show results of where the accreted gas comes from and how it can move through the gap. We discuss the results in Sect. 7

2. Model setup

To model the migration and accretion of embedded planets in disks we use 2D locally isothermal models that are calculated with the hydrodynamical code NIRVANA (Ziegler & Yorke 1997; Ziegler 1998). We use a setup that would, without a planet, represent an accreting equilibrium disk including a mass flow onto the central star with constant accretion rate $\dot{m}$. The initial and boundary conditions are identical to our simulations in Dürmann & Kley (2015). Therefore, the disk surface density is given by

$$\Sigma(r) = \frac{\dot{m}}{3\pi\alpha h^2\sqrt{GM_\odot}} r^{-1/2} = \Sigma_0 r^{-1/2}, \tag{1}$$

and the initial radial velocity is

$$u_r = u_r^{\mathrm{visc}} = -\frac{3}{2}\alpha h^2 r\Omega_\mathrm{K}, \tag{2}$$

where Ω_K is the Keplerian orbital frequency and u_r^{visc} is the speed of the radial viscous flow for an equilibrium disk with constant $\dot{m}$. The outer boundary conditions are a forced inflow at a constant $\dot{m}$ with the initial radial velocity. At the inner boundary we have a forced outflow with the initial radial velocity and zero gradient for the density and energy density. The computational domain covers the region between $r_\mathrm{min} = 0.3r_0$ and $r_\mathrm{max} = 3.0r_0$ with $r_0 = 5.2$ au, and $\Sigma_0 = \Sigma(r_0)$. At the inner boundary there is a damping region between r_min and $1.25r_\mathrm{min}$ where all components of the velocity are damped to the azimuthal average with increasing strength closer to the boundary. At the outer boundary the damping region begins at $0.8r_\mathrm{max}$ and there the $\tau_{r,r}$ element of the stress tensor is increased for the radial velocity update to suppress the viscous overstability (Kley et al. 1993). We resolve the domain with 389 radial and 901 azimuthal equally spaced grid cells. The planet is introduced on a circular orbit at $a_0 = r_0 = 5.2$ au around a solar mass star. The viscosity is given by the α-model with $\alpha = 0.003$ and the disk scale height is $h = 0.05$.

In the first 500 orbits, corresponding to approximately 6000 years, the planet is held on its initial circular orbit to allow the disk time to adapt to the presence of a massive planet. During this phase, the planet opens a gap in the disk as would happen during a slow growth process in the disk. We do not reach full equilibrium in this 6000 years but, because we are interested in migration, the main goal is to make sure the disk is able to adapt to the migrating planet without introducing strong artificial effects as a result of the sudden release. Another method we use to reduce the effects of the release of the planet is to slowly switch on the disk torques acting on the planet over six orbits.

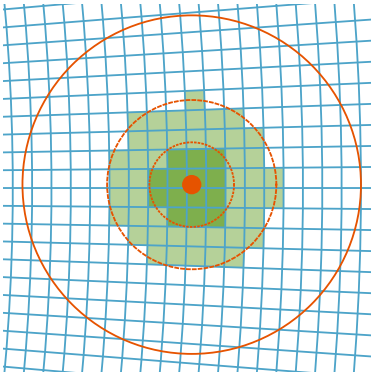

Fig. 1. Section of the grid around a planet (red dot) and its Hill Radius R_H shown as a red circle. The smaller dashed circles have radii of $R_\mathrm{H}/2$ and $R_\mathrm{H}/4$. The accretion mechanism we use removes gas from the lighter and darker shaded cells. In the darker shaded cells the accretion fraction is increased by a factor of two. Because the planet is allowed to move in the grid it is not centered in a cell or located on cell boundaries.

The torques generated within $f_\mathrm{t} = 0.8R_\mathrm{H}$ are reduced applying a Fermi-like tapering function

$$f_\mathrm{taper}(r_\mathrm{cell}) = \frac{1}{1+\exp\left(-\frac{r_\mathrm{cell}-f_\mathrm{t}}{0.1f_\mathrm{t}}\right)}, \tag{3}$$

where r_cell is the distance of the cell to the planet. The total torque is then calculated by

$$\Gamma_\mathrm{tot} = \sum_\mathrm{cells} f_\mathrm{taper}(r_\mathrm{cell})\Gamma_\mathrm{cell}\,, \tag{4}$$

where Γ_cell is the torque exerted by one grid cell on the planet. This way gas which is already bound to the planet does not contribute to the migration

3. Accretion method

To model the mass accretion onto the planet we rely on the method already used in our previous work (Dürmann & Kley 2015), originally described by Kley (1999), but with some refinements. At each time-step the gas density in cells within half of the Hill radius $R_\mathrm{H} = a_\mathrm{P}\,(M_\mathrm{P}/3M_*)^{1/3}$ around the planet is reduced by a fraction $f_\mathrm{acc}\Delta t\Omega$ where a_P is the semimajor axis of the planet, Δt is the time step, Ω the Keplerian orbital frequency at the initial planetary orbit, and the accretion fraction f_acc is a free parameter. In addition, the accretion in the inner quarter of the Hill radius is twice as high as in the outer quarter, as explained in Fig. 1. Tanigawa & Watanabe (2002) showed that the accretion rate converges for a fixed f_acc if the accretion zone is small enough, $\lesssim 0.07R_\mathrm{H}$, but as we are interested in modeling different accretion rates and our method is not realistic anyhow, we chose a larger region, which is beneficial for a smooth accretion rate with a planet moving through the grid. The parameter, f_acc, defines a depletion timescale, at which the affected cells in the Hill sphere will be emptied if there is no flow of gas refilling them. From the accretion fraction the depletion timescale can be calculated by $\tau_\mathrm{acc} = (f_\mathrm{acc}\Omega)^{-1}$ which gives the timescale at which the inner part of the Hill sphere would be emptied as $\rho = \rho_0\exp(-t/\tau_\mathrm{acc})$ if it would not be refilled by surrounding

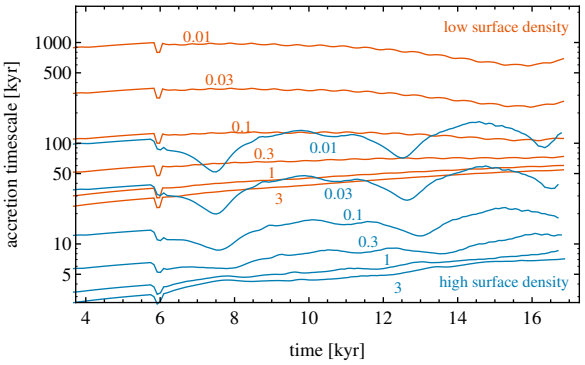

Fig. 2. Accretion timescale for Jupiter-mass planets with different accretion fractions $f_{\rm acc}$ given as numbers close to the lines. For the first 6000 years the planets were on fixed orbits and their mass kept constant, while already gas was removed in the vicinity of the planet. Then the planets began to migrate and the gas removal was continued, but it was not added to the mass of the planet. The models were calculated with surface density $\Sigma_0 = 88\,\mathrm{g/cm^2}$ (red) and $\Sigma_0 = 880\,\mathrm{g/cm^2}$ (blue), respectively.

gas. The mass removed this way is measured and either added to planet mass or not, depending on the particular model. Increasing the planet's mass affects its dynamical mass as well as the gravitational potential. In calculations where we include a tracer gas it can be accreted the same way as the gas and the amount of removed tracer is measured separately.

In addition to the mass accretion, we also take the possibility of momentum accretion into account in our models. In the simplest assumption, the specific linear and angular momentum of the planet is not affected by the increased mass, thus the velocity of the planet in the disk is not modified by accretion. But the accreted gas, depending on its position in the disk, may have a relative velocity with respect to the planet and therefore this simple assumption does not hold necessarily. To account for this, we measure the linear momentum of the removed gas in each cell and can add its sum to the linear momentum of the planet as we increase its mass. This way we avoid taking into account the rotation (spin) of the planet around its own axis and ensure conservation of linear momentum. Obviously the linear momentum and the orbital angular momentum of the planet are strongly coupled, so if the planet changes its linear momentum this way, it will also change its orbital angular momentum around the star.

4. Accretion without growth

Our model of accretion depends on the choice of an appropriate accretion fraction, f_{acc}, that cannot be derived from physical arguments in our simulations. To model these processes, one would need a very high spatial grid resolution close to the planet and additional physics such as thermodynamics, radiation transport, opacities and even chemistry. This is not in the scope of this work and for this reason we chose another approach. To find a value of the accretion fraction that leads to accretion rates consistent with previous work we performed a parameter study. We place a Jupiter-mass planet in disks with two different surface densities of $88\,\mathrm{g\,cm^{-2}}$ and $880\,\mathrm{g\,cm^{-2}}$ at 5.2 au corresponding to $\dot{m} = 10^{-8}$ and $10^{-7}\,\mathrm{M_\odot\,yr^{-1}}$, respectively. For the accretion fractions, $f_{\rm acc}$, we chose values between 10^{-2} and 3. We only removed the gas in the vicinity of the planet from the simulation but its mass was kept constant in this first series of models studied in this section. The effect of a mass change of the planet is studied in the following section.

For our chosen accretion method a higher disk surface density should lead to a higher accretion rate onto the planet. In Fig. 2 we show the accretion timescale $\tau = m_{\rm P}/\dot{m}_{\rm P}$ obtained in these calculations. In case of low accretion fractions the accretion timescales are directly proportional to the depletion timescale $\tau \propto \tau_{\rm acc} = (f_{\rm acc}\Omega)^{-1}$, and the inverse of the disk surface density. A factor of ten in the accretion fraction or the surface density reduces the accretion timescale to 10 %, hence the blue and red lines are offset initially by a factor of ten. For very high accretion fractions this proportionality no longer holds due to the accretion timescale reaching a lower limit because in this case the disk is not able to supply any more gas to the planet. Because the amount of gas still depends on the disk mass for the different surface densities, the accretion timescale limits are again approximately a factor of ten apart. The lower limit of the timescale is approximately 20 kyr for the low density disk and approximately 3 kyr for the high density disk, which is in agreement with Lubow et al. (1999), D'Angelo et al. (2002) and Machida et al. (2010).

The accretion timescale is not constant with time, but changes during the different phases of the simulations. During the first phase of the simulations where the planet is held on a fixed circular orbit the accretion timescale gets larger, meaning slower accretion. This can be explained by the introduction of the planet into the undisturbed disk. The planet begins to carve a gap and the density near the planet is reduced slowing down the accretion until a new equilibrium is reached. After 6000 years the planet is released and allowed to migrate which is the cause of the small perturbations in all the curves at this time.

In this second phase the accretion timescale does not behave as smoothly as before. This is best seen for the calculations with higher disk density (blue lines) as there are visible valleys at 7.5, 12.5 and 16.5 kyr in Fig. 2, that move to slightly later times for smaller accretion timescales. As the planets are migrating with different rates, these valleys appear in all calculations when the planets are at specific positions in the disk, which are $a_{\rm P} = 0.88, 0.67$ and $0.55\,r_0$, as can be seen clearly in Fig. 3 where the valleys appear as bumps. This also holds true for the simulations with lower surface densities, where the migration is much slower and only the valley at $a_{\rm P} = 0.88$ is visible at approximately 15.5 kyr. In Fig. 3, which shows the same models as Fig. 2, but for the highest and lowest accretion fraction, the bump at $a_{\rm P} = 0.67$ is also visible.

To identify the origin of these variations we ran additional simulations where we changed various parameters of the models. We found that the location of the bumps dependend on the location of the inner boundary, that is, the value of $r_{\rm min}$, but not on the value of $r_{\rm max}$. The position does not depend on the numerical resolution and is independent of the initial position of the planet. However, we found some dependence on the strength of the damping at $r_{\rm min}$ because the damping changes the position of the effective inner boundary felt by the planet. The position of the bumps also depends on the boundary condition (open or closed inner boundary) and on the sound speed in the disk. Here, a higher disk aspect ration h shifts the bumps to smaller radii and vice versa. This suggests that the features might be related to sound wave reflections by the inner boundary and their interaction with the migrating planet but future work is needed to investigate this effect in detail. The increase of the accretion rate is caused by an increased density in a region very close to the planet ($|\boldsymbol{r} - \boldsymbol{r}_{\rm P}| \lesssim R_{\rm H}/2$) while the global structure of the disk is unchanged. This also explains why the bumps disappear for

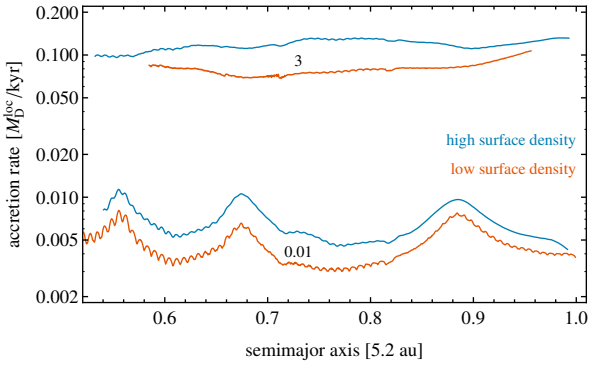

Fig. 3. Accretion rate for selected models from Fig. 2 (measured in units of the local disk mass $M_D^{loc} = a_P^2 \Sigma_0 a_P^{-1/2}$ per kyr) as a function of the planet's distance. Only the highest and lowest accretion fractions (numbers) are shown. The red and blue lines correspond to low and high surface density.

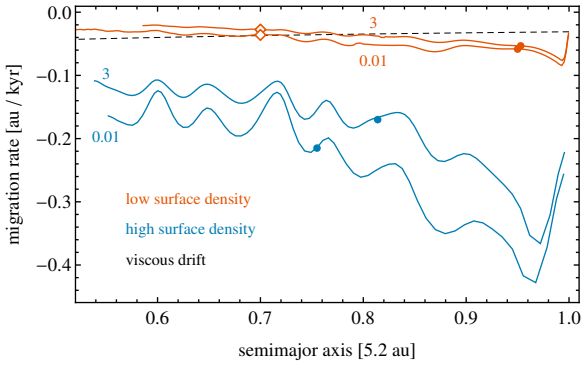

Fig. 4. Migration rates of the simulations shown in Fig. 3. The black dashed line is the radial viscous flow speed for an equilibrium disk with constant $\dot{m}$ (see Eq. 2), which is independent of the surface density. The dots and diamonds mark those times in the evolution which are discussed in section 6 and Fig. 13

higher accretion fractions. If the accretion is strong enough, no build-up of gas close to the planet is possible. The variation of the accretion timescale is in all cases a factor of approximately two. At the moment we do not fully understand this effect, but it does not influence the overall global evolution of the disk. Our additional calculations show no significant variations in the torques (and thus the migration rate) for different values of the damping, the location of the inner boundary (within reasonable limits) or the size of the damping region. The migration rates in Fig. 4 show no correlation with the accretion rate in Fig. 3. As we are mainly interested in comparing the migration behavior of the planet at different accretion rates, the absolute values of accretion may differ without invalidating our results.

The accretion rate depending on the planet's position in the disk is displayed in Fig. 3. The accretion rate is given in local disk masses $M_D^{loc} = \Sigma_0 a_P^{3/2}$ per kyr to compare the accretion rate of the different surface densities. The main difference remaining is that the planet in the more massive disk (blue line) is migrating much faster as can be seen in Fig. 4. The higher migration rate of the planet leads to a higher accretion rate, because more gas can be supplied to the Hill sphere. The accretion rates onto the planet in the high accretion limit exceed the viscous accretion rate of the disk onto the star by a factor of approximately five in the beginning, reducing to a factor of two after 11000 years of evolution. We already discussed the fact that planets do not migrate at the equilibrium viscous speed but can be faster or slower in Dürmann & Kley (2015).

Accreting planets migrate slower, as shown in Fig. 4. In case of the high accretion rate limit ($f_{acc} = 3$) it is slowed down by up to 30 % compared to the slow accretion with $f_{acc} = 0.01$ (which does not differ in migration rate from non-accreting simulations) for both high and low surface density. In the models discussed in this section the mass of the planet was not increased during the migration. Therefore, the changes in the migration rate due to different accretion rates are only an effect of the reduced surface density because of the gas removal from the Hill sphere. The lower density reduces the torques and as a result slows down the migration and in a more massive disk this effect will be stronger because more mass can be removed.

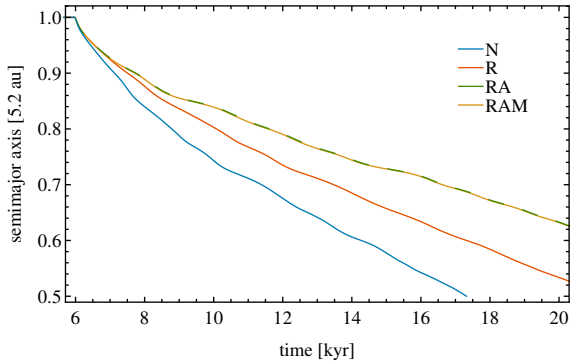

Fig. 5. Orbital evolution of an initially Jupiter-mass planet. In model R the gas is only removed, but not added to the planet's mass. In model RA the gas is accreted and increases the planet's mass and in RAM the linear momentum of the accreted gas is also added to the planet. Model N is for comparison, no gas is removed in the vicinity of the planet. Model RA and RAM are very similar so they are plotted as dashed lines.

5. Models with mass growth

In addition to the previous models, in order to understand the influence of the planetary mass accretion on the migration of massive planets we compared different methods of accretion. For comparison reasons, in the first model we only removed the gas near the planet and did not add it to the planet (model named R), as in the models discussed in section 4. In the following run we added it to the planet mass and kept the specific linear momentum constant (RA) and in the last one we added it and also the linear momentum of the removed gas to the planet (RAM). As a reference, we also ran calculations where we did not even remove the gas from the simulation (N). To estimate the maximum possible effect, we chose the accretion fraction $f_{acc} = 3.0$, which is in the saturated upper limit of the accretion rate and the disk surface density $\Sigma_0 = 880\,\mathrm{g\,cm^{-2}}$. In the first 6000 years (500 orbits) the planets are held on circular orbits and, while the gas is already removed from the simulation, the mass is kept constant at $M_P = M_{Jup}$. Then the accretion is switched on (according to the respective model) and the planets move according to their interaction with the gas disk.

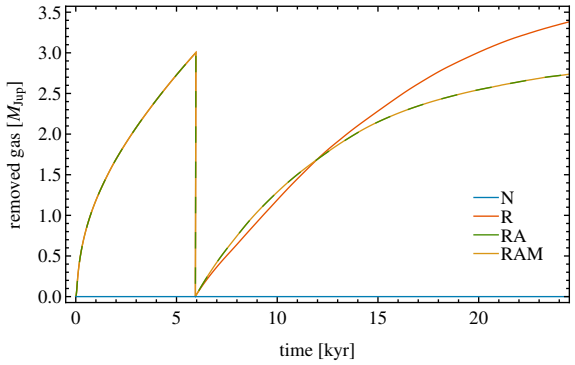

Fig. 6. Removed gas for the different models considered in Fig. 5. Before the migration is switched on at 6000 years the planets do not increase their mass and behave like model R in order to start the evolution with 1 $M_{\rm Jup}$. After the release, we reset the counter and in models RA and RAM the mass is now increased according to the removed gas. Again the line of model RA is shown as a dashed line to show model RAM behind.

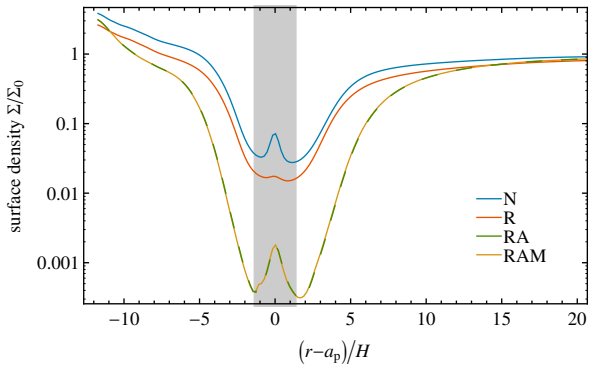

Fig. 7. Surface density profile close to the planet for the different models discussed in Sec. 5 when the planet has reached $a_{\rm p} = 0.75 r_0$. The distance to the planet is given in units of the local disk scaleheight. The shaded region shows the radial extent of the Hill radius.

The evolution of the semimajor axis in the different models is shown in Fig. 5. Directly after the release of the planets, the disk has still to adapt to the now moving planet. This transition is smoothed by gradually switching on the torques acting onto the planet over six orbits. After a few 100 years the disk has adapted to the moving planet, and the planet and the disk bear no history of the migration to that point, which we tested by releasing the planet from circular orbits with different initial radii.

In Fig. 6 we show the amount of gas removed in the vicinity of the planet. During the first phase where the planet is on a fixed circular orbit the accretion is very high in the beginning as the slope is nearly vertical. At this time the planet begins to carve a gap in the disk and the density in its vicinity is still high. As soon as the gap develops, the slope decreases and the accretion becomes slower. The mass of the planet is not increased until the planet is free to migrate, but in Fig. 6 we show the amount of removed gas up to that time. The higher amount of removed gas for the models where the mass of the planet is increased is a result of the higher mass of the planet. Since the Hill sphere is growing with the planet's mass, the accretion is enhanced in the beginning, but as the gap is deepened it reduces the amount of

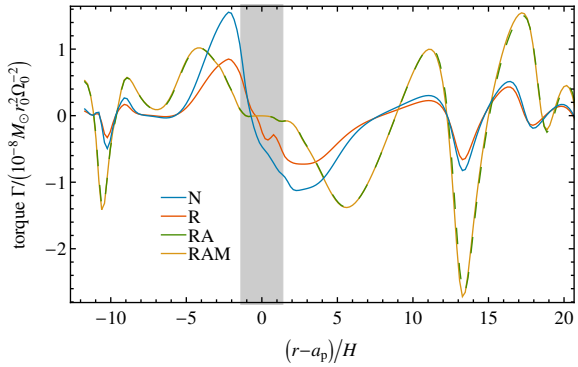

Fig. 8. Torque profile close to the planet similar to Fig. 7. Note that the excluded torques (see Eq. 3) are not shown in this graph. Torques inside the shaded region are from outside the Hill sphere (e.g., the horseshoe region).

material close to the planet and accretion is slowed down again. After 25 kyr the planets reached a mass of 2.8 $M_{\rm Jup}$ (RA) and 3.4 $M_{\rm Jup}$ (R) which is in agreement with results by Nelson et al. (2000).

The migration rates of the different models vary significantly. Fastest is the migration without gas removal or accretion (model N). We show the surface density close to the planet in Fig. 7 at times where the planets have reached $a_{\rm p} = 0.75 r_0$ (see Fig. 5). Because no gas is removed, the overall surface density is increased compared to the model R and also gas accumulates close to the planet. For models RA and RAM, due to the more massive planet, the density in the gap is less than 10 % of that in model R. Similarly, we show the radial torque profile in Fig. 8. Models N and R significantly differ only within $5H$ of the planet, resulting from the higher surface density. This means model R has to migrate slower than model N. Models RA and RAM show identical torques and differ from the other models because the planet at this time has nearly tripled its mass and thus produces stronger torques. Because the more massive planet at the same time needs stronger torques to be moved, but these torques do not increase as much because the gap becomes deeper, the net effect is a slower migration.

The models RA and RAM are indistinguishable by eye in all these calculations. When a planet is accreting gas it also has to accrete momentum, otherwise the increased mass at constant momentum would lead to a decreasing velocity, which of course is unphysical. The main contribution to the accreted momentum is the orbital momentum, which is very similar for the planet and the gas because they are both nearly on Keplerian orbits. However, there are also deviations from this mean motion such as in- or outflow, as in the horseshoe orbits. These deviations are captured by the momentum accretion in the RAM models while the RA models handle only the mean motion. In Fig. 9 we show the total torque acting on the planet (disk forces & accreted momentum) as well as the torque resulting from accreted momentum which is not orbital momentum. The contribution of the momentum accretion to the total torque is less than 5 % at the beginning and at later times very small (less than 0.5 %) and therefore negligible. Because we cannot resolve the circumplanetary disk, our models do not consider the angular momentum of the removed gas with reference to the planet to analyze its rotation.

During the evolution, the eccentricity of the planetary orbit does not increase significantly and is below 0.006 at all times. We also monitored the eccentricity of the disk which was well

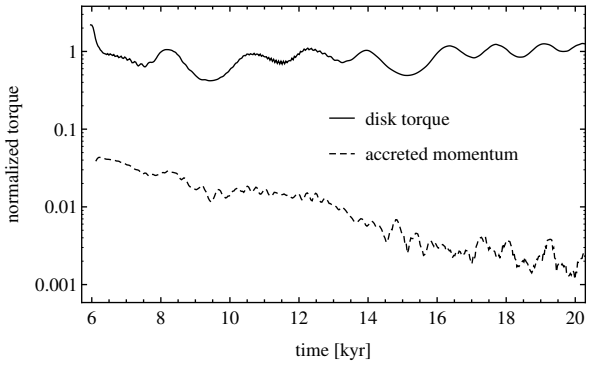

Fig. 9. Total disk torque in the RAM model from the disk (solid line) and the accreted momentum (dashed line) acting on the planet, normalized to its average. The line for the accreted momentum shows only the deviations from the orbital momentum because the orbital momentum does not influence the migration of the planet.

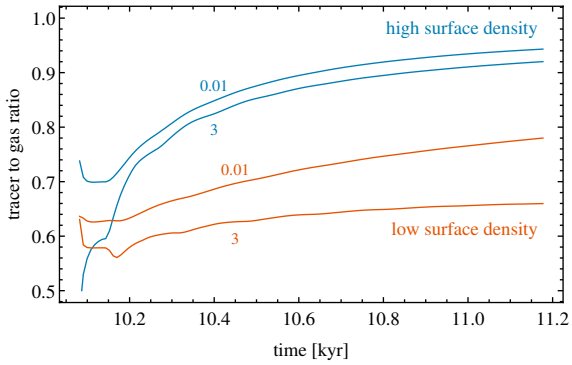

Fig. 10. Fraction of the accreted tracer to the accreted gas $m_{\rm acc}^{\rm tracer}/m_{\rm acc}^{\rm gas}$. The different colors correspond to high and low accretion rates and high and low disk density.

below 0.015 during the calculations. For all simulations shown in this paper, the gap edges were steady and displayed no oscillations or eccentricities.

6. Origin of accreted gas

To investigate the origin of the accreted gas, we implemented a tracer fluid, which is advected with the gas in the simulation. It can therefore be removed from the simulation as the accreted gas and the total amount of removed tracer fluid is measured. After 10000 years, when the disk had ample time to adapt to the planet and its accretion and migration, we introduced the tracer fluid. These times in the orbital evolution are marked in Fig. 4 by round dots. The tracer has the same distribution as the gas, but is only present inside the planet's current orbit. By measuring the accreted tracer and comparing it to the accreted gas we can determine whether the accreted material comes from the area inside the planet's orbit or from the area outside the planet's orbit. Because the planet is migrating during the simulation and therefore inner and outer parts of the disk are mixing and changing with time, we restrict this kind of analysis to 1000 years after the introduction of the tracer gas. To account for different migration rates, we used two different disk surface densities of 88 and 880 g cm^{-2} , and in both cases we considered accretion near the high limit found in section 4 with $f_{\rm acc} = 3$ and in the non saturated case with $f_{\rm acc} = 0.01$.

The ratio $m_{\rm acc}^{\rm tracer}/m_{\rm acc}^{\rm gas}$ is shown in Fig. 10 where $m_{\rm acc}^{\rm gas}$ and $m_{\rm acc}^{\rm tracer}$ are the amount of gas and tracer accreted by the planet after the tracer introduction. The ratio is between 0.5 and 0.75 in the beginning but then increases. The initial increase is due to the initial distribution which is not in equilibrium because of the flow pattern in the gas, as is the case for horseshoe orbits. In case of the more massive disk, which also implies a faster migration rate after only 300 years, more than 80 % of the accreted material is originating from the inner disk. In the end, the ratio for both accretion fractions is well above 90 %. Even for the low disk density, and the, therefore, slower migrating planets, the ratio is almost always above 60 %. The planets in simulations with higher surface density are migrating much faster as can be seen in Fig. 4. The planets in the simulations with higher surface density both migrate approximately $0.03r_0$ while in case of the lower surface density they move only $0.01r_0$ during the 1000 years with the tracer. Because they traveled much less than the gap width, they have not migrated far into the initially inner disk. This means the planet is still at the edge of the tracer fluid and the ratio of accreted tracer to gas is not only a result of the planets migration deep into the region with the tracer fluid. In case of the lower accretion rate more material comes from the inner disk than for the higher accretion rate. To understand this behavior, we analyzed the density distribution of the tracer material in the vicinity of the planet.

In Fig. 11 the evolution of the tracer with time is shown for the low surface density models in Fig. 10. While for the low accretion rate (upper row) gas crosses the gap and accumulates outside the planets orbit, in case of high accretion of the planet, the tracer is only transported in the horseshoe region (lower row). After 240 years the outermost horseshoe orbit is already completely populated with tracer material and with increasing time it only becomes more homogeneous, while for the low accretion rate the region containing tracer is increasing.

In Fig. 12 we show the surface density of the tracer zoomed in to the vicinity of the planet 950 years after the tracer in the inner disk was introduced. In addition to the models in Fig. 11 the calculations with high surface density are also shown. In the models with low accretion in the top row a pile-up of gas at the position of the planet is clearly visible, but in case of high accretion it nearly completely vanishes. The tracer in all cases shows the spiral structure generated by the planet into the outer disk. The models in the right column have a higher surface density, thus the planets migrate faster, and because the migration is faster than the viscous radial speed of the gas in all four models at this time (see Fig. 4), the material passes the gap from the inner to the outer disk and accumulates outside the gap. In the simulations with the lower surface density, the migration is still faster than the radial viscous speed but slower compared to the higher density models and hence the transport of material from the inner to the outer disk is slowed down. Some transport of material from the inner to the outer disk will of course occur in any case, and even without migration because it is transported through the horseshoe region as shown in Fig. 11. This mechanism can also be seen in the lower left panel of Fig. 12 where some gas has accumulated in horseshoe orbits and follows their bending near the planet, but there is no pile up of gas outside the horseshoe region. This means all the material from the inner disk is accreted onto the planet and also explains why the ratio of accreted tracer to gas in Fig. 10 for that case is reduced compared to the lower accretion rate. The material from the inner

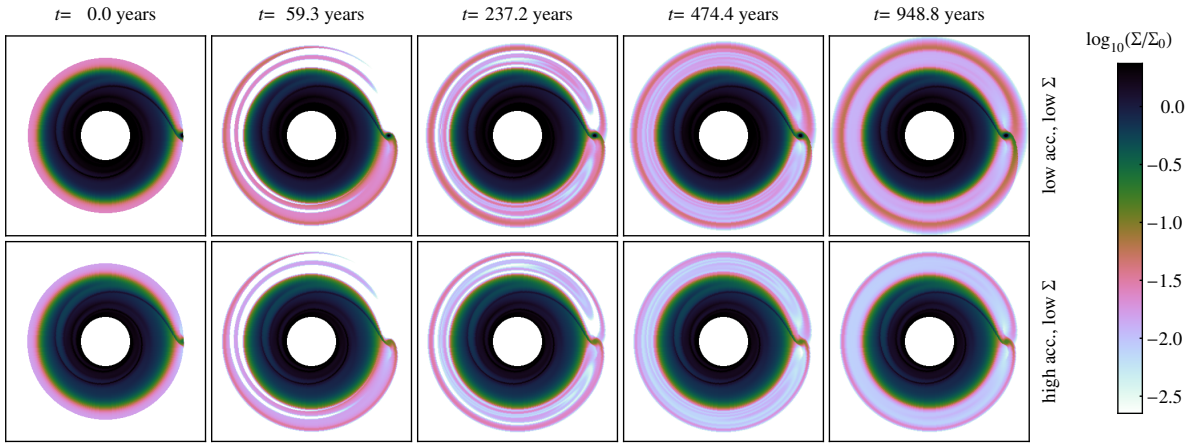

Fig. 11. Tracer density at different times after the tracer was introduced in the simulation. Both rows show the low surface density (88 g cm^{-2}) with low accretion fraction $f_{\rm acc} = 0.01$ in the upper and $f_{\rm acc} = 3.0$ in the lower row. These models correspond to the low surface density models in Fig. 10.

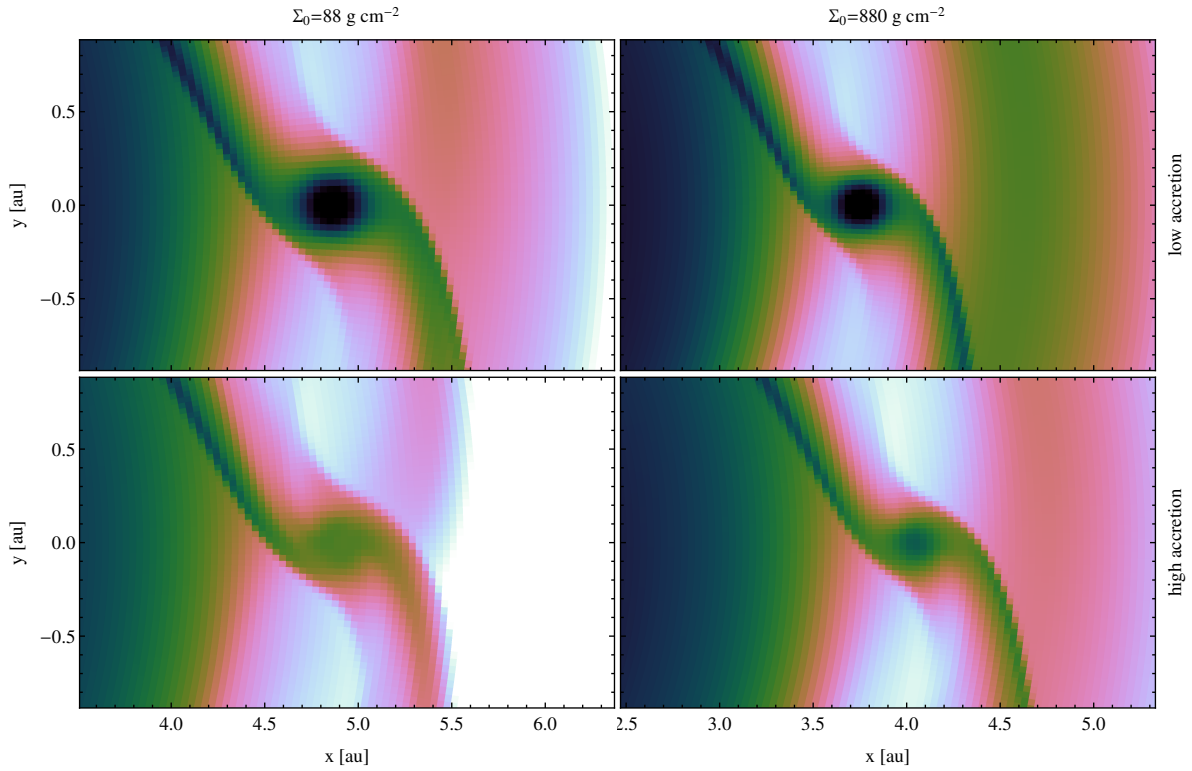

Fig. 12. Tracer fluid density near the planet 950 years after the tracer introduction to the inner disk. The four panels show the density distribution for low (88 g cm^{-2}) and high (880 g cm^{-2}) disk density from left to right and low ($f_{\rm acc} = 0.01$) and high ($f_{\rm acc} = 3$) accretion rate from top to bottom. The color map is the same as in Fig. 11.

disk alone is not enough to refill the Hill sphere so there has also to be a flow of gas from the outer disk. The same happens, but to a much lesser extent, for the higher disk density where the ratio in the case of the higher accretion fraction is also decreased. This can be better understood by looking at the disks local $\dot{m}$ profile shown in Fig. 13.

The $\dot{m}$ measures the mass change in the disk by radial movement of gas, therefore a negative $\dot{m}(r)$ means mass from that annulus in the disk is moving inwards, and vice versa with a positive $\dot{m}(r)$. The $\dot{m} = -10^{-8}\, M_\odot$/yr at the outer domain boundary is a parameter of the simulation and corresponds to the specified value used in Eq. (1). It would also be the global $\dot{m}$ of the disk in equilibrium without a planet or a non-accreting planet

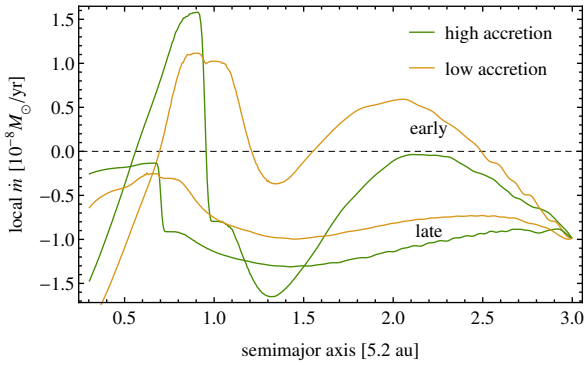

Fig. 13. $\dot{m}$-profile of the disk (negative values mean inward transport) for several models of the low density case and thus with prescribed disk accretion rate $-10^{-8}\,M_\odot$/yr (see. Eq. 1). The profiles are averaged over 1000 years, because they are very sensitive to small disturbances. The different colors correspond to the models with high (green) and low (yellow) accretion fractions at early (t = 10 kyr) and late times (t = 44 kyr) in the evolution. The times are marked with red dots and diamonds in Fig. 4. The planets early in the evolution are migrating much faster than the viscous speed, in the later models they migrate slower than the viscous speed. The jumps at the planet position correspond to the accretion onto the planet, which is therefore much higher in the green lines.

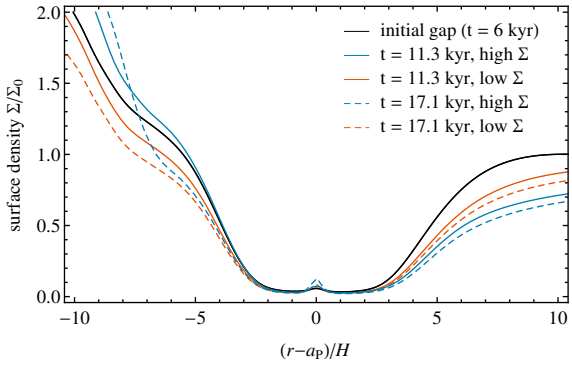

Fig. 14. Normalized surface density profiles for planets with low accretion rate ($f_{\rm acc}$ = 0.01) at different times during their orbital evolution. The horizontal axis is normalized to the planet's position and the disk scale height. The black line corresponds to the surface density when the planets are released.

on a fixed circular orbit. This was shown in Dürmann & Kley (2015) (their Fig. 4), where one can see that reaching the equilibrium takes very long even without the planet migrating. There we also found the initial outward motion of the disk material in outer parts of the disk as seen here in Fig. 13. These only disappeared after very long times (> 3600 orbits or 43 kyr) even for a fixed, non-migrating planet, which is consistent with these features disappearing for the late models in our new simulations as presented here. For the models with high accretion rate (green) there is a jump at the position of the planet, because the planet is removing gas at that position. When $\dot{m}$ is always negative close to the planet (as in the late models) this means that, although the planet is accreting and migrating, gas is crossing from the outer disk to the inner disk, and vice versa for the early model with low accretion (yellow), where the gas close to the planet is moving outwards through the gap. Also clearly visible is that a fast migrating planet can have a strong impact on the local value of $\dot{m}$ in the whole disk and even induce outward drift of the gas far away from its position. The important part explaining the difference in the fraction of accreted material from the inner disk depending on the accretion rate can be seen immediately outside (right) of the planets position. For both early and late times, the local $\dot{m}$ for the high accretion models is significantly lower than for the low accretion models and negative meaning a gas flow directed toward the planet. Because the planet wants to accrete more gas, the Hill sphere has to refill, and although in most models gas is crossing the gap inside out, the inward gas flow at the outer gap edge is stronger, leading to a higher fraction of gas from the outer disk.

6.1. Relation to type II migration

Our simulations show that gas can cross the gap carved by a giant planet and does so, for example, in cases where the planet is migrating faster than the viscous radial speed. If the planet is migrating inward faster than the disk, most material will originate from the inner disk. Only for high accretion rates and, at the same time, sufficiently low disk surface densities, will the planet be able to accrete all of the gas transported through the gap, as seen in the lower left panel of Fig. 12. Only in these special cases does the gap impose a barrier between the inner and outer gap and the planet would be in the classical type II regime. Also in these cases, however, the migration rate can differ from the classical type II migration rate because this is given by the global equilibrium value, which can differ from the actual local value, as for the example seen in Fig. 13.

It seems plausible that phases of type II regime can be reached by a migrating planet for a wider range of surface densities and accretion rates, but only as a transient state. If the planet is migrating inwards faster than $u_r^{\rm visc}$ and is accreting a considerable amount of the gas crossing the gap inside out, the surface density at the outer gap edge will be slightly reduced which is shown in Fig. 14. Because the outer gap edge exerts a negative torque leading to inward migration, a lower density in this region will slow down migration. But at the time when the migration rate equals $u_r^{\rm visc}$ the outer gap edge is still depleted and the migration rate will continue to slow down. This means, although the radial viscous speed is somehow a natural migration rate, a massive gap opening planet will usually migrate faster or slower if it did not happen to begin its evolution in already perfect equilibrium. Due to the fact that, during the overall evolution of planets, the migration transits from fast type I migration or even faster type III migration, this perfect equilibrium seems highly unlikely.

7. Conclusions

Our simulations show that the disk sets a limit on how much gas can be supplied to the Hill sphere and thus can be accreted by the planet. The upper limit of the accretion rate onto the planet is higher than the accretion rate through the disk onto the star by a factor of five or less , and reduces with time, which agrees with findings of Kley (1999) and Tanigawa & Tanaka (2016).

We show that there are some reciprocal effects between accretion and migration. Migration is fastest in the unphysical case where no gas is removed. In this case gas is accumulating near the planet and generating large torques because of the small distance to the planet. Removal of gas close to the planet reduces these torques and slows down the migration. When gas is re-

moved and the planet increases its mass, the migration slows down even more. Not only is the gas density close to the planet reduced because of the removal of gas but also because the now more massive planet creates a deeper gap. In addition, a growing planet needs stronger torques to keep up its migration rate, but the torque created in the gap region becomes smaller together with the reduced density. Also, as a result of the deeper gap, the accretion rate can drop below the accretion rate of a much lighter planet, which does not increase its mass. We not only increased the mass of the planet, but also measured the momentum of the removed gas and added it to the planet. The simulation clearly shows that this accreted momentum does not have a noticeable effect on the migration of the planet, as the torque it generates is always smaller by a factor of 100 compared to the disk torques responsible for the migration.

The models with tracer particles to investigate the origin of accreted material gave multiple interesting results. For a planet migrating faster than the radial viscous speed (i.e., faster than type II migration), most of the accreted gas originates from the inner disk and this fraction increases when the planet is migrating faster. In this case it does not push the inner disk, but gas crosses the gap from the inner to the outer disk. Only in cases of high accretion rates and low enough surface densities is the planet able to accrete all of this material. In cases where the planet is migrating slower than the viscous speed gas crosses the gap from the outer to the inner disk. In both cases gas is able to cross the gap, so it is not separating the inner and the outer disk. The rate at which gas crosses the gap is determined by the migration rate of the planet. It can be, and often is, faster than the radial viscous speed of the disk which is the local type II migration rate in the disk.

When the planet is migrating at exactly the viscous speed, and is therefore in the classical type II migration, this is only a transient state during its orbital evolution. As we show in Fig. 4 the migration rate is higher in the beginning but then drops and reaches the viscous drift rate. However, the migration rate is dropping further and becomes even lower than the viscous speed. Also, whether or not gas crosses the gap depends not only on the model parameters but also on changes with time, as can be seen in Fig. 13. The actual migration rate is defined by the state of the disk on both sides of the gap whose evolution depends on a local viscous timescale, which can be different from the global viscous timescale.

To find the relations that describe the actual migration rate for a given system, further work is needed. For the whole picture it is very important not to neglect the influences of accretion and migration on one another. The former cannot be understood without a better understanding of the second, and vice versa. The migration history, which results in varying accretion rates during the evolution, and the origin of accreted material, may be reflected in the planet's composition, and allow a better understanding of the late formation. This has to be studied in population synthesis models, which include more detailed models of the mutual effects of migration and accretion. Analytical models for planet growth such as Tanigawa & Ikoma (2007) that do not include the planet migration, will underestimate the final masses of planets because they do not account for the gas crossing the gap and entering the Hill sphere. In agreement with previous studies (Nelson et al. 2000) we find that masses of several Jupiter masses can be reached if single massive planets are allowed to migrate undisturbed through their disks.

Finally we note that in our simulations we modeled only 2D locally isothermal disks. It will be worthwhile in the future to extend these to full 3D.

Acknowledgements. We want to thank Aurélien Crida and Bertram Bitsch for many useful discussions and helpful critisism. Some of the numerical simulations were performed on the bwGRiD cluster in Tübingen, which is funded by the state of Baden-Württemberg, and the cluster of the Forschergruppe FOR 759 funded by the DFG. The work of Christoph Dürmann was sponsored with a scholarship of the Cusanuswerk.

References

Baruteau, C., Crida, A., Paardekooper, S.-J., et al. 2014, Protostars and Planets VI, 1, 667
Baruteau, C. & Masset, F. 2013, in Tides in Astronomy and Astrophysics (Springer), 201–253
Duffell, P. C., Haiman, Z., MacFadyen, A. I., D'Orazio, D. J., & Farris, B. D. 2014, ApJ, 792, L10
Dürmann, C. & Kley, W. 2015, A&A, 574, A52
D'Angelo, G., Henning, T., & Kley, W. 2002, A&A, 385, 647
D'Angelo, G., Kley, W., & Henning, T. 2003, ApJ, 586, 540
Edgar, R. G. 2007, ApJ, 663, 1325
Fung, J., Shi, J.-M., & Chiang, E. 2014, ApJ, 782, 88
Hasegawa, Y. & Ida, S. 2013, ApJ, 774, 146
Hubickyj, O., Bodenheimer, P., & Lissauer, J. J. 2005, Icarus, 179, 415
Kley, W. 1999, MNRAS, 303, 696
Kley, W. & Nelson, R. 2012, ARA&A, 50, 211
Kley, W., Papaloizou, J., & Lin, D. 1993, ApJ, 409, 739
Lin, D. & Papaloizou, J. 1986, ApJ, 309, 846
Lubow, S., Seibert, M., & Artymowicz, P. 1999, ApJ, 526, 1001
Machida, M. N., Kokubo, E., Inutsuka, S.-i., & Matsumoto, T. 2010, MNRAS, 405, 1227
Morbidelli, A. & Crida, A. 2007, Icarus, 191, 158
Nelson, R. P., Papaloizou, J. C., Masset, F., & Kley, W. 2000, MNRAS, 318, 18
Paardekooper, S.-J. 2014, MNRAS, 444, 2031
Pierens, A. & Raymond, S. N. 2016, MNRAS, 462, 4130
Pollack, J. B., Hubickyj, O., Bodenheimer, P., et al. 1996, Icarus, 124, 62
Tanigawa, T. & Ikoma, M. 2007, ApJ, 667, 557
Tanigawa, T. & Tanaka, H. 2016, ApJ, 823, 48
Tanigawa, T. & Watanabe, S.-i. 2002, ApJ, 580, 506
Ward, W. 1982, in Lunar and Planetary Science Conference, Vol. 13, 831–832
Ziegler, U. 1998, Computer Physics Communications, 109, 111
Ziegler, U. & Yorke, H. W. 1997, Computer Physics Communications, 101, 54

4 Results

During the work for this thesis two papers, referenced herein as P1 and P2, were published. The first one, *Migration of massive planets in accreting disks*, was published in January 2015 in the refereed journal Astronomy & Astrophysics. In the paper the migration rate of planets with different masses is simulated in isothermal disks with varying density and viscosity and the torques acting on the planet are analyzed in detail. The second paper, *The accretion of migrating giant planets*, was accepted for publication in October 2016 and is currently in press also in Astronomy & Astrophysics. In this piece the effect of gas accretion and the gas flow into and across the gap is studied.

In P1 we first studied the properties and shape of a gap with a planet on a fixed circular orbit and showed we could simulate a disk with a radial accretion flow prescribed as a parameter of the model. We measured the torques of this configuration and later compared it to the values of a migrating planet. This showed that it is necessary to actually model migration because the analysis of static torques is not sufficient and yields different migration rates. It became clear that the disk must adapt to the effects of a migrating planet and that both gap and torque change compared to the static model. As soon as the disk has adapted the gap profile and the specific torques do not change and do not depend on the position of the planet in the disk (see Fig. 8 and Fig. 9 in P1). This implies that also the total torques, normalized by the known type I torque normalization as in Eq. 1.5, acting on the planet have to become constant after the disk has adapted to the planet migration (see Fig. 13 in P1). This is a strong argument against the classical type II migration principle where the torques will always adjust themselves to keep the planet aligned in the middle of the gap moving with the viscous radial speed u_r^{visc}.

According to Eq. 1.9 type II migration cannot be faster than the viscous radial speed and is only slowed down if the planet mass exceeds the local disk mass. This contradicts with the results in the first paper and was also found by Duffell et al. (2014) where the migration can be faster or slower than the viscous evolution (see Fig. 15 in P1). To investigate how this happens we measured how the disk material is transported radially in and close to the gap. The local disk accretion rate profile of an inward migrating planet

(see Fig. 11 in P1) clearly shows positive values meaning outward gas flow because the planet is migrating faster than the viscous speed of the disk. We could not only show that gas can cross the gap but also that even an outward flow is possible given the planet is migrating inward faster than the viscous radial speed of the gas in the undisturbed disk. Would no gas be able to cross the gap all the gas inside the planet's orbit would accumulate at the inner gap edge like snow pushed by a snowplough. This would then create stronger torques pushing the planet back. A gas flow across the gap on the other hand means type II migration is essentially not working as thought before.

In P2 we investigated in more detail the effects of planetary gas accretion on the migration. The method used to accrete gas from the disk allows for adjusting the accretion rate with a parameter given as a model parameter. This method cannot model all physical aspects of accretion like gravitational heating and circumplanetary disks but allows to easily adjust the accretion rate. This way we cannot determine the actual accretion rate a planet would have but at least find an upper limit of the accretion rate (or a lower limit to the accretion timescale). Apart from that we were able to analyze the effect of accretion by increasing or decreasing the accretion rate in otherwise identical models. The simulations show that accretion, normalized to the disk density, is faster if the planet migrates faster. The reason is, because gas can flow through the gap and more gas flows through the gap if the planet is migrating faster, more gas is transported into the Hill sphere where it can be accreted by the planet (see Figs. 3 and 4 in P2).

As an accreting planet constantly increases its mass, the disk adapts to the more and more massive planet which has the effect that the evolution of planets at different times in their evolution can hardly be compared. Hence, up to this point we did not increase the planet's mass, although gas was removed, in order to not change too many variables at the same time. This is of course unphysical so we added models where the effect of a growing planet could be analyzed. Apart from the gas accretion we also accounted for the momentum of the accreted gas and considered its influence on the migration of the planet. For example, if the specific momentum of the accreted gas was lower than that of the planet this would increase the inward migration rate. Our computations show (see Fig. 5 in P2) that in case of no gas removal at all the planet migrates the fastest followed by the case where gas is only removed, but the planet does not grow. The migration becomes slowest if the planet is allowed to grow but the momentum of the removed gas is not important (see Fig. 9 in P2). The reason for the slowed down migration of the accreting and growing models is that the gap becomes deeper because of the gas removal and thus the torques are reduced compared to the model without gas removal

(see Fig. 7 and Fig. 8 in P2). If in addition the planet becomes heavier this makes the gaps even deeper and also a more massive planet needs stronger torques to migrate at the same rate. Because the growing planet migrates slower and the gap becomes deeper it will also have a reduced accretion rate and eventually will accrete gas much slower than the less massive planet (see Fig. 6 in P2).

To further investigate the gas flow across the gap also for accreting planets we introduced a tracer fluid into the simulation. The tracer replicates the density distribution on the gas in the inner disk and is zero everywhere in the outer disk. Because the tracer behaves the same way as the gas and can also be accreted by the planet this way we were able to measure how the material from the inner and the outer disk mixes and which fraction of the accreted gas originates in the inner and outer disk. The simulations show that a planet migrating faster than the viscous drift rate will accrete most of the gas from the inner disk as gas will cross the gap from the inner disk to the outer disk (see Fig. 10 and Fig. 13 in P2). Also analyzed was whether gas not just flows into the gap but crosses the gap and reaches the other side, although the planet is accreting. In Fig. 12 of P2 tracer material accumulates outside the planets horseshoe region even for the highest possible accretion rate. Only if at the same time the disk is not very dense all gas can be accreted. It is important to note that we used the maximum accretion rate that is possible and the accretion rate in more realistic models will be lower.

All the results presented in the publications summarized here show that the idea of type II migration is not what happens when massive planets migrate. The actual process is much more complicated with feedback effects of the migration itself and the accretion onto the planet.

5 Discussion

The results presented in this thesis shed a new light on type II migration. Massive planets fundamentally influence the formation process of all planets in an emerging planetary system. Hence, the understanding of their migration should be considered to create a complete model of planet formation. Although this work does not yield a fundamental understanding how migration of massive planets work it has shown the classical idea of type II migration is not valid and does not explain what is happening during migration.

It is clearly necessary to investigate the migration process further and in even more detail than it could be done for this thesis. Our models were isothermal and 2-dimensional and therefore could not resolve the accretion onto the planet with the 3-dimensional flow pattern in a circumplanetary disk and gravitational heating of the accreted gas. It would be worthwhile to extend the simulations to full 3-dimensional radiative hydrodynamics to include the thermodynamics of accretion and thus be able to further constrain how fast accretion onto the planet happens. Another problem is the resolution of the region close to the planet. `NIRVANA` supports nested grids with up to 10 layers of refinement but as these nested grids are at fixed locations in the highest-level grid they cannot be used to model a radially moving planet. Other codes can use adaptive mesh refinement that increases the resolution of dynamically identified regions of interest and thus would allow to increase the local resolution. However, as the planet moves through the disk the region which has to be refined constantly changes which limits the increase in resolution because constantly interpolation has to be used. A possible solution could be a grid which is dynamically rescaled to the radial position of the planet as discussed in the dissertation of Paardekooper et al. (2006, section 4.2). This method allows for the planet to be stationary in the grid although it is able to migrate. Combined with nested grids this could overcome the problems stated above with the additional benefit that the computational domain could be smaller without the planet eventually reaching the inner boundary as it moves along with the planet.

With new and better telescopes like ALMA (Atacama Large Millimeter/submillimeter Array) it now becomes possible to observe the structure of protoplanetary disks. The

well-known image of HL Tau shows clear axisymmetric features that immediately were discussed as possible gaps of multiple forming giant planets among other theories. Although it is not yet clear if the rings in the disk around HL Tau are signatures of forming planets, it is highly interesting to have the possibility to observe planetary gaps as this allows to validate planet formation theory not only with statistics of finished planetary systems but by direct observations. Because ALMA is observing in millimeter and submillimeter wavelengths unfortunately the gas is not visible. The images show only the dust in the disk and it is difficult to reconstruct the gas distribution. However, the first time being able to look at the evolution of protoplanetary disks, will with no doubt fuel the interest in the planet-disk-interactions and the most important kind of these is planet migration.

Other telescopes that will be able to help understanding planet formation are planned. One of them is the James Webb Space Telescope (JWST), which is scheduled to launch in 2018 for infrared wavelengths. The European Extremely Large Telescope (ELT) as well as the Thirty Meter Telescope (TMT) will be used for infrared and optical observations starting service (scheduled) in 2024. Both can be used for direct imaging of exoplanets around nearby stars and may allow for spectroscopy of planetary atmospheres. The PLATO satellite mission (PLAnetary Transits and Oscillation of stars) of ESA will continue the research of Kepler and CoRoT to detect undiscovered exoplanets and is scheduled for launch in 2024. In contrast to Kepler, which observed a single far away region of the Milky Way to have many stars in a single field of view, PLATO will focus on stars closer to the sun. This will make spectroscopic follow-up observations possible with other telescopes to measure not only the radius of the planet by transits but also the masses by radial velocity measurements and possibly also atmospheric properties by absorption spectroscopy of starlight traveling through the planet's atmosphere. Other spacecraft missions focusing on the detection, confirmation and further observation of exoplanets are the TESS (Transiting Exoplanet Survey Satellite) mission and the CHEOPS (CHaracterising ExOPlanets Satellite) space telescope.

In the context that type II migration is considered to be too fast to replicate the observations with population synthesis models this work is promising as some of our models were slower than the viscous drift rate. With already more than 20 citations for the first publication we raised the awareness that migration of giant planets is a field of research where still much work is to be done.

Acknowledgements

Doing research is almost never the result of one person working alone, but a constant process of discussion, exchange of ideas and solving problems together. The same is true with the research that resulted in this thesis. I want to thank my supervisor Willy Kley for uncounted occasions where with just a single sentence he spared me hours of searching for papers with the one information I needed, for true and honest curiosity in what I did, and of course the many discussions which helped me to find a way through code, data and nearly 4 years of researching. I thank Moritz Stoll for helping me navigating the perils of Linux, various shells and compilers and for often lending an eye (or two) when something seemed too good or really bad. I enjoyed being part of the Computational Physics group.

I am very grateful the Cusanuswerk funded 3 years of my PhD (in addition to the 3 years during my Bachelor and Master studies), allowing me to follow this topic without the need to put effort in earning money. In addition, I gathered an incredible variety of experiences and got to know so many interesting, helpful and simply nice people (and I am happy to call a lot of them ”friends”).

Special thanks go to my family, especially my parents, for all the support and encouragement I received during all these years. I want to thank all my friends, because they motivated me to keep working but also helped me to spend time for recreation.

Last but not least I thank those people, especially Benedikt, who helped me to write this thesis and find many typos and unclear or wrong formulations.

Bibliography

Armitage, P. (2010). *Astrophysics of Planet Formation*. Cambridge University Press.

Balbus, S. A. & Hawley, J. F. (1991). A powerful local shear instability in weakly magnetized disks. I-Linear analysis. II-Nonlinear evolution. *The Astrophysical Journal*, 376, 214–233.

Baruteau, C., Crida, A., Paardekooper, S.-J., Masset, F., Guilet, J., Bitsch, B., Nelson, R., Kley, W., & Papaloizou, J. (2014). Planet-Disk Interactions and Early Evolution of Planetary Systems. *Protostars and Planets VI*, 1, 667–689.

Bitsch, B. & Kley, W. (2011). Range of outward migration and influence of the disc's mass on the migration of giant planet cores. *Astronomy & Astrophysics*, 536, A77.

Cieza, L., Padgett, D. L., Stapelfeldt, K. R., Augereau, J.-C., Harvey, P., Evans, N. J., Merín, B., Koerner, D., Sargent, A., Van Dishoeck, E. F., et al. (2007). The Spitzer c2d survey of weak-line T Tauri stars. II. New constraints on the timescale for planet building. *The Astrophysical Journal*, 667(1), 308.

Crida, A., Morbidelli, A., & Masset, F. (2006). On the width and shape of gaps in protoplanetary disks. *Icarus*, 181(2), 587–604.

Desch, S. (2007). Mass distribution and planet formation in the solar nebula. *The Astrophysical Journal*, 671(1), 878.

Duffell, P. C., Haiman, Z., MacFadyen, A. I., D'Orazio, D. J., & Farris, B. D. (2014). The Migration of Gap-opening Planets is Not Locked to Viscous Disk Evolution. *The Astrophysical Journal Letters*, 792(1), L10.

Edgar, R. G. (2007). Giant planet migration in viscous power-law disks. *The Astrophysical Journal*, 663(2), 1325.

Gammie, C. F. (2001). Nonlinear outcome of gravitational instability in cooling, gaseous disks. *The Astrophysical Journal*, 553(1), 174.

General Assembly of the IAU (2006). Result of the IAU Resolution votes. http://www.iau.org/news/pressreleases/detail/iau0603/.

Goldreich, P. & Tremaine, S. (1979). The excitation of density waves at the Lindblad and corotation resonances by an external potential. *The Astrophysical Journal*, 233, 857–871.

Haisch, Jr., K. E., Lada, E. A., & Lada, C. J. (2001). Disk frequencies and lifetimes in young clusters. *The Astrophysical Journal Letters*, 553(2), L153.

Hartmann, L., Calvet, N., Gullbring, E., & D'Alessio, P. (1998). Accretion and the evolution of T Tauri disks. *The Astrophysical Journal*, 495(1), 385.

Hasegawa, Y. & Ida, S. (2013). Do Giant Planets Survive Type II Migration? *The Astrophysical Journal*, 774(2), 146.

Hayashi, C. (1981). Structure of the solar nebula, growth and decay of magnetic fields and effects of magnetic and turbulent viscosities on the nebula. *Progress of Theoretical Physics Supplement*, 70, 35–53.

Hunger, H., Reade, J., & Parpola, S. (1992). *Astrological Reports to Assyrian Kings*. Number Bd. 8 in Astrological Reports to Assyrian Kings. Helsinki University Press.

Johansen, A., Blum, J., Tanaka, H., Ormel, C., Bizzarro, M., & Rickman, H. (2014). The Multifaceted Planetesimal Formation Process. *Protostars and Planets VI*, 1, 547–570.

Kley, W. & Nelson, R. (2012). Planet-Disk Interaction and Orbital Evolution. *Annual Review of Astronomy and Astrophysics*, 50, 211–249.

Latham, D. W., Stefanik, R. P., Mazeh, T., Mayor, M., & Burki, G. (1989). The unseen companion of HD114762-A probable brown dwarf. *Nature*, 339, 38–40.

Lin, D. & Papaloizou, J. (1979). Tidal torques on accretion discs in binary systems with extreme mass ratios. *Monthly Notices of the Royal Astronomical Society*, 186(4), 799–812.

Lin, D. & Papaloizou, J. (1986). On the tidal interaction between protoplanets and the protoplanetary disk. III-Orbital migration of protoplanets. *The Astrophysical Journal*, 309, 846–857.

Lin, D. & Papaloizou, J. (1993). On the tidal interaction between protostellar disks and companions. In *Protostars and Planets III* (pp. 749–835).

Lin, D. N., Bodenheimer, P., & Richardson, D. C. (1996). Orbital migration of the planetary companion of 51 Pegasi to its present location.

Masset, F. & Papaloizou, J. (2003). Runaway migration and the formation of hot Jupiters. *The Astrophysical Journal*, 588(1), 494.

Matzner, C. D. & Levin, Y. (2005). Protostellar disks: formation, fragmentation, and the brown dwarf desert. *The Astrophysical Journal*, 628(2), 817.

Mayor, M. & Queloz, D. (1995). A Jupiter-mass companion to a solar-type star. *Nature*, 378, 23.

Mizuno, H. (1980). Formation of the giant planets. *Progress of Theoretical Physics*, 64(2), 544–557.

Nelson, R. P., Gressel, O., & Umurhan, O. M. (2013). Linear and non-linear evolution of the vertical shear instability in accretion discs. *Monthly Notices of the Royal Astronomical Society*, (pp. stt1475).

Owen, J. E., Ercolano, B., & Clarke, C. J. (2011). Protoplanetary disc evolution and dispersal: the implications of x-ray photoevaporation. *Monthly Notices of the Royal Astronomical Society*, 412(1), 13–25.

Paardekooper, S.-J. et al. (2006). *Growing and moving planets in disks*. PhD thesis, Leiden Observatory, Faculty of Mathematics and Natural Sciences, Leiden University.

Rafikov, R. R. (2009). Properties of gravitoturbulent accretion disks. *The Astrophysical Journal*, 704(1), 281.

Raymond, S., Kokubo, E., Morbidelli, A., Morishima, R., & Walsh, K. (2014). Terrestrial Planet Formation at Home and Abroad. *Protostars and Planets VI*, 1, 595–618.

Shakura, N. I. & Sunyaev, R. A. (1973). Black holes in binary systems. Observational appearance. *Astronomy and Astrophysics*, 24, 337–355.

Shu, F. H., Johnstone, D., & Hollenbach, D. (1993). Photoevaporation of the solar nebula and the formation of the giant planets. *Icarus*, 106(1), 92–101.

Skrutskie, M., Dutkevitch, D., Strom, S. E., Edwards, S., Strom, K. M., & Shure, M. A. (1990). A sensitive 10-micron search for emission arising from circumstellar dust associated with solar-type pre-main-sequence stars. *The Astronomical Journal*, 99, 1187–1195.

Stoll, M. H. & Kley, W. (2014). Vertical shear instability in accretion disc models with radiation transport. *Astronomy & Astrophysics*, 572, A77.

Tanaka, H., Takeuchi, T., & Ward, W. R. (2002). Three-dimensional interaction between a planet and an isothermal gaseous disk. I. Corotation and Lindblad torques and planet migration. *The Astrophysical Journal*, 565(2), 1257.

Toomre, A. (1964). On the gravitational stability of a disk of stars. *The Astrophysical Journal*, 139, 1217–1238.

Walsh, K. J., Morbidelli, A., Raymond, S. N., O'Brien, D. P., & Mandell, A. M. (2011). A low mass for Mars from Jupiter's early gas-driven migration. *Nature*, 475(7355), 206–209.

Ward, W. (1982). Tidal barriers in the solar nebula. In *Lunar and Planetary Science Conference*, volume 13 (pp. 831–832).

Weidenschilling, S. & Cuzzi, J. N. (1993). Formation of planetesimals in the solar nebula. In *Protostars and planets III* (pp. 1031–1060).

Wolszczan, A. & Frail, D. A. (1992). A planetary system around the millisecond pulsar PSR 1257+ 12. *Nature*, 355(6356), 145–147.

Ziegler, U. & Yorke, H. W. (1997). A nested grid refinement technique for magnetohydrodynamical flows. *Computer Physics Communications*, 101(1), 54–74.